AMERICAN SOCIETY FOR MICROBIOLOGY | Journal of Virology®

VIRUS-CELL INTERACTIONS

Ruxolitinib and Polycation Combination Treatment Overcomes Multiple Mechanisms of Resistance of Pancreatic Cancer Cells to Oncolytic Vesicular Stomatitis Virus

Sébastien A. Felt, Gaith N. Droby, Valery Z. Grdzelishvili

Department of Biological Sciences, University of North Carolina at Charlotte, Charlotte, North Carolina, USA

ABSTRACT Vesicular stomatitis virus (VSV) is a promising oncolytic virus (OV). Although VSV is effective against a majority of pancreatic ductal adenocarcinoma cell (PDAC) cell lines, some PDAC cell lines are highly resistant to VSV, and the mechanisms of resistance are still unclear. JAK1/2 inhibitors (such as ruxolitinib and JAK inhibitor I) strongly stimulate VSV replication and oncolysis in all resistant cell lines but only partially improve the susceptibility of resistant PDACs to VSV. VSV tumor tropism is generally dependent on the permissiveness of malignant cells to viral replication rather than on receptor specificity, with several ubiquitously expressed cell surface molecules playing a role in VSV attachment to host cells. However, as VSV attachment to PDAC cells has never been tested before, here we examined if it was possibly inhibited in resistant PDAC cells. Our data show a dramatically weaker attachment of VSV to HPAF-II cells, the most resistant human PDAC cell line. Although sequence analysis of low-density lipoprotein (LDL) receptor (LDLR) mRNA did not reveal any amino acid substitutions in this cell line, HPAF-II cells displayed the lowest level of LDLR expression and dramatically lower LDL uptake. Treatment of cells with various statins strongly increased LDLR expression levels but did not improve VSV attachment or LDL uptake in HPAF-II cells. However, LDLR-independent attachment of VSV to HPAF-II cells was dramatically improved by treating cells with Polybrene or DEAE-dextran. Moreover, combining VSV with ruxolitinib and Polybrene or DEAE-dextran successfully broke the resistance of HPAF-II cells to VSV by simultaneously improving VSV attachment and replication.

IMPORTANCE Oncolytic virus (OV) therapy is an anticancer approach that uses viruses that selectively infect and kill cancer cells. This study focuses on oncolytic vesicular stomatitis virus (VSV) against pancreatic ductal adenocarcinoma (PDAC) cells. Although VSV is effective against most PDAC cells, some are highly resistant to VSV, and the mechanisms are still unclear. Here we examined if VSV attachment to cells was inhibited in resistant PDAC cells. Our data show very inefficient attachment of VSV to the most resistant human PDAC cell line, HPAF-II. However, VSV attachment to HPAF-II cells was dramatically improved by treating cells with polycations. Moreover, combining VSV with polycations and ruxolitinib (which inhibits antiviral signaling) successfully broke the resistance of HPAF-II cells to VSV by simultaneously improving VSV attachment and replication. We envision that this novel triple-combination approach could be used in the future to treat PDAC tumors that are highly resistant to OV therapy.

KEYWORDS DEAE-dextran, combination treatment, oncolytic virus, pancreatic cancer, Polybrene, polycation, resistance, vesicular stomatitis virus, virus attachment, type I interferon, ruxolitinib

Received 20 March 2017 **Accepted** 19 May 2017

Accepted manuscript posted online 31 May 2017

Citation Felt SA, Droby GN, Grdzelishvili VZ. 2017. Ruxolitinib and polycation combination treatment overcomes multiple mechanisms of resistance of pancreatic cancer cells to oncolytic vesicular stomatitis virus. J Virol 91:e00461-17. https://doi.org/10.1128/JVI.00461-17.

Editor Douglas S. Lyles, Wake Forest University

Address correspondence to Valery Z. Grdzelishvili, vzgrdzel@uncc.edu.

Oncolytic virus (OV) therapy is an anticancer approach that uses replication-competent viruses that can selectively infect, replicate in, and kill cancer cells. Currently, three OVs are approved for clinical use: herpes simplex virus 1-based talimogene laherparepvec (T-Vec [Imlygic]) for melanoma, approved in the United States (1) and later in the European Union (2); enteric cytopathic human orphan virus 7-based Rigvir for melanoma, in Latvia, Georgia, and Armenia (3); and adenovirus type 5-based Gendicine and Oncorine for head and neck squamous cell carcinoma in China (4).

This study focuses on vesicular stomatitis virus (VSV) (a rhabdovirus), which has been used successfully against many cancers in preclinical studies (5, 6) and is currently in a phase I clinical trial against refractory solid tumors (ClinicalTrials.gov registration numbers NCT02923466, NCT03120624, and NCT03017820). The oncoselectivity of VSV is generally based on the type I interferon (IFN)-associated antiviral potential of target cells. Although VSV cannot distinguish nonmalignant (here called "normal") cells from cancer cells based on their receptor profile or cell cycle, there is a large difference between normal and cancer cells in their abilities to sense and respond to viral infection (7). When normal cells are infected with VSV, viral infection is sensed by normal cells, and the production of type I IFNs is triggered to impede viral replication and spread via the induction of an antiviral state in infected cells as well as in the noninfected tissue surrounding the IFN-producing cells. In contrast, a majority of tumors have inhibited or defective type I IFN signaling (8–11), likely because many IFN responses are antiproliferative, antiangiogenic, and proapoptotic (12). As VSV is highly sensitive to type I IFN responses, it therefore preferentially replicates in cancer cells. The oncoselectivity of wild-type (WT) VSV is not sufficient, as it is able to inhibit type I IFN signaling through one of the functions of the VSV matrix (M) protein, which localizes to the nuclear envelope and inhibits the nucleocytoplasmic trafficking of cellular mRNAs, thus impeding antiviral gene expression not only in cancer but also normal cells (13). As a result, WT VSV exhibits intolerable toxicity, most notably neurotoxicity (7). Thus, intranasal administration of VSV in rodents can result in fatal infection of the central nervous system (14), and in nonhuman primates, intrathalamic administration results in severe neurological disease (15). To address this safety issue, various recombinant VSVs with dramatically improved safety and oncoselectivity profiles have been generated (5).

One of the well-known features of VSV is its pantropism (7), with several ubiquitously expressed cell surface molecules, such as the low-density lipoprotein (LDL) receptor (LDLR) (16), phosphatidylserine (17–19), sialoglycolipids (20), and heparan sulfate (21), suggested to play a role in VSV attachment to host cells. While such pantropism does not allow VSV to distinguish normal cells from cancer cells based on their differential receptor expression profiles, the relative independence of VSV on a single receptor can be an advantage, allowing VSV-based OVs to target a wide range of tumor types. In contrast, other OVs could be limited by the expression of their receptor, such as the coxsackievirus and adenovirus receptors required for the efficient entry of widely used adenovirus type 5-based OVs (22).

This study focuses on pancreatic ductal adenocarcinomas (PDACs), which comprise approximately 95% of pancreatic cancers. Standard cancer therapies show little efficacy in treating PDAC (23), and PDAC is expected to become the second leading cause of cancer-related deaths in the United States by 2030 (24). Different OVs have been tested against PDAC *in vitro* and *in vivo*, with various efficacies (25). Our recent studies demonstrated that VSV is effective against the majority of human PDAC cell lines, both *in vitro* and *in vivo* (26). However, some PDAC cell lines are highly resistant to VSV infection, at least in part due to their upregulated type I IFN signaling and constitutive expression of a subset of interferon-simulated genes (ISGs) (26–29). We have shown that the treatment of resistant PDAC cell lines with type I interferon inhibitors, such as JAK inhibitor I (a pan-JAK inhibitor) or ruxolitinib (a specific JAK1/2 inhibitor), significantly improves the permissiveness of these cells to VSV (27–29). However, this approach only moderately improved the susceptibility of resistant cells to initial VSV infection, and overall VSV replication never reached the level of VSV-permissive PDAC

cell lines (27–29). In agreement with this observation, pretreatment of cells with ruxolitinib (compared to posttreatment only) did not change the kinetics of VSV replication, with a significant increase in VSV replication that could be seen only at 48 h postinfection (p.i.), even in cells pretreated with ruxolitinib for up to 48 h, suggesting that ruxolitinib did not improve the rate of initial infection but rather facilitated secondary infection via the inhibition of antiviral signaling in PDAC cells (28, 29).

Together, data from our previous studies suggest that resistant PDAC cell lines may have an additional block at an early stage of VSV infection that cannot be removed via JAK inhibition. In this study, we examine the role of VSV attachment in the resistance of PDAC cells to VSV, as it is the first critical stage for successful VSV infection. We show that inefficient VSV attachment can contribute to the resistance of PDACs to VSV. Moreover, we successfully used a novel approach to break the multiple mechanisms of resistance of PDAC cells to VSV by combining the virus with polycations and ruxolitinib to simultaneously improve VSV attachment and virus replication.

RESULTS

VSV attachment to HPAF-II cells is impaired. The human PDAC cell line HPAF-II, which showed the highest level of resistance to VSV in our previous studies, was the main focus of this study (26–30). In addition, many experiments included Hs766T, another VSV-resistant human PDAC cell line, as well as two VSV-permissive human PDAC cell lines, MIA PaCa-2 and Suit2. This work focuses on one of the most commonly used VSV-based oncolytic recombinants, VSV-ΔM51 (here called VSV; the figure legends and Materials and Methods indicate the specific VSV recombinant used in each experiment), which has a deletion of a methionine at position 51 in the matrix (M) protein (31). This mutation causes an ablation of the ability of the WT M protein to inhibit cellular antiviral gene expression. As many cancers have defective type I interferon antiviral signaling, VSV-ΔM51 can still replicate in and kill cancer cells (32, 33). In addition, to facilitate the visualization of viral infection, VSV recombinants used in this study encode either the near-infrared red fluorescent protein (RFP) (34) or green fluorescent protein (GFP) (31) open reading frame (ORF) inserted between the VSV G and L genes.

We used two different approaches to examine the efficacy of VSV attachment to PDAC cells. For fluorescence-activated cell sorter (FACS) analysis, virus attachment was examined by using cells in suspension (Fig. 1A). Adherent cells were treated with EDTA to detach them from plastic surfaces, incubated with different amounts of VSV (multiplicity of infection [MOI] of 1.25 or 12.5 based on the VSV titer determined on MIA PaCa-2 cells) for 1 h at 4°C, washed to remove any unbound virus, and analyzed for cell-bound VSV by using VSV-G antibody and FACS analysis. EDTA, rather than trypsin, was used to retain protein receptors of VSV (such as LDLR) on the cell surface. We also assayed VSV attachment using an alternative approach, where VSV attachment to cell monolayers was examined. Cells were incubated with different amounts of VSV (MOI of 0.1 to 250 based on the titer determined on MIA PaCa-2 cells) for 1 h at 4°C, washed to remove any unbound virus, and analyzed for cell-bound VSV by using Western blot analysis of the total cell lysates (Fig. 1B). As our study focuses on attachment, for both approaches, virus-cell incubations were conducted at 4°C to prevent virus entry. To confirm that VSV did not penetrate cells under these conditions, cells were incubated with VSV for 1 h at 4°C, trypsinized to remove all surface proteins, and analyzed for the presence of VSV. As expected, no VSV products were detected after trypsinization, indicating that VSV was bound to the cell surface only (data not shown).

As shown in Fig. 1A for VSV attachment to cells in suspension, the lowest level of VSV attachment (percentage of VSV-positive cells as well as the mean fluorescence intensity [MFI]) was observed in HPAF-II cells under both tested conditions (MOIs). For example, at an MOI of 12.5, only 10% of HPAF-II cells were VSV positive, compared to 57.4% of Hs766T cells, 31.9% of MIA PaCa-2 cells, and 46.5% of Suit2 cells. In agreement with these data, we also observed lower levels of VSV attachment to HPAF-II cell monolayers (Fig. 1B). Based on the serial dilutions of virus and comparison of VSV

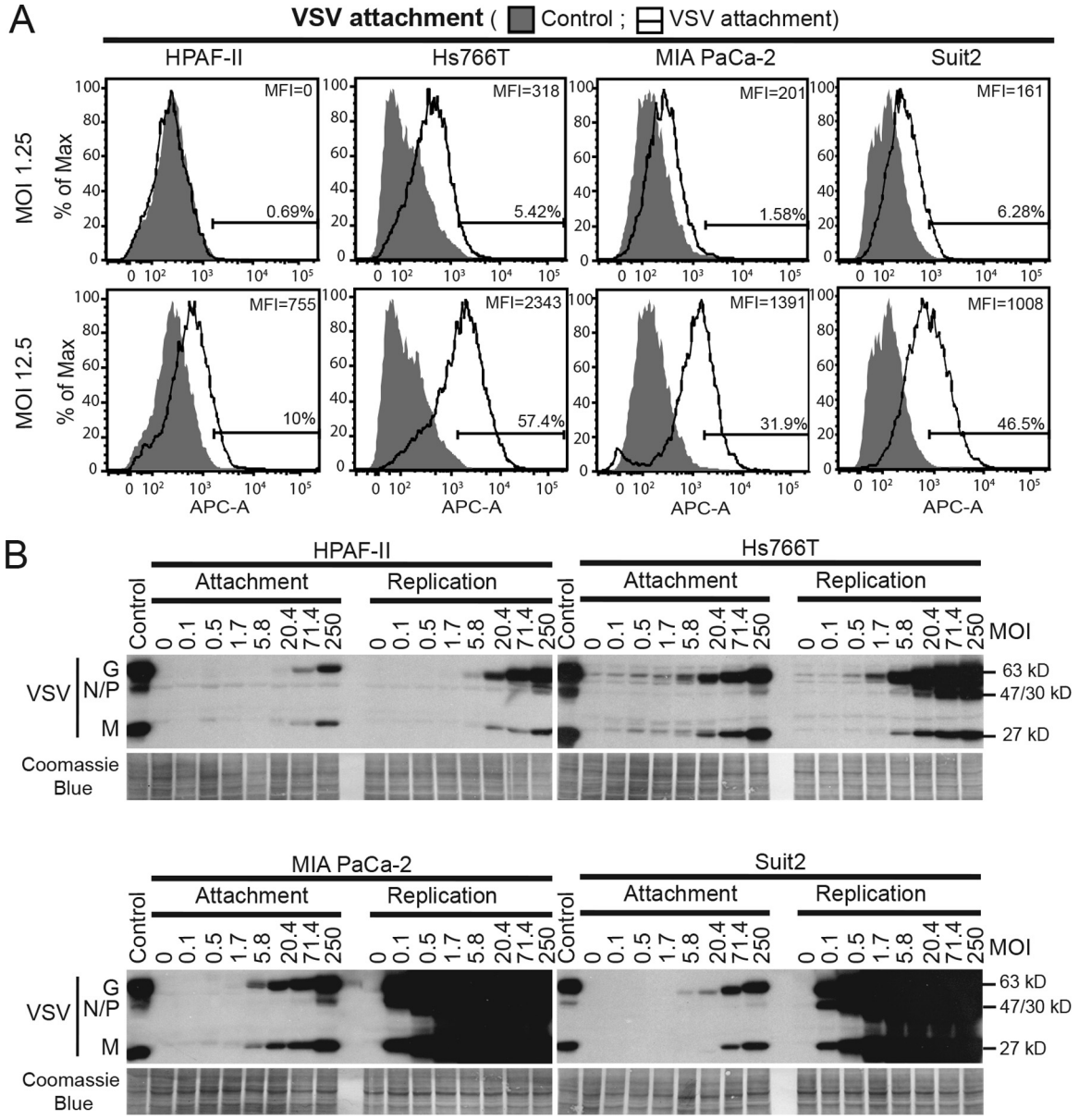

FIG 1 VSV attachment to PDAC cell lines. (A) For VSV attachment to cells in suspension, cells were detached with PBS with 0.2% EDTA and incubated with VSV-ΔM51-eqFP650 for 1 h at 4°C. After incubation with VSV-G primary antibody and APC-conjugated secondary antibody, cells were analyzed by FACS analysis using the APC-A channel. "Control" cells were mock treated (without VSV), and primary and secondary antibodies were used. "VSV attachment" cells were incubated with various amounts of VSV (the indicated MOIs are based on virus titration on MIA PaCa-2 cells). Gated populations are positive for VSV attachment (the percentage of VSV-positive cells is indicated above the gate line). The MFI for each population was calculated by using FlowJo software (TreeStar). (B) For VSV attachment to cells in monolayers, cell monolayers were incubated with VSV-ΔM51-eqFP650 for 1 h at 4°C ("Attachment") or for an additional 8 h at 37°C ("Replication"). Protein was isolated and analyzed by Western blotting. The MOI is indicated at the top and is based on virus titration on MIA PaCa-2 cells. Protein product sizes (kilodaltons) are indicated on the right. Coomassie blue stain was used to indicate equal loading.

protein bands of similar intensities for each cell line, VSV was attaching to HPAF-II cells at least 12-fold less efficiently than to MIA PaCa-2 and Hs766T cells and 3.5-fold less efficiently than to Suit2 cells (Fig. 1B). During examination of VSV attachment to cell monolayers, a duplicate set of samples was incubated for an extra 8 h at 37°C to determine relative VSV replication levels and confirm the status of PDAC cell lines in regard to their resistance/permissiveness to VSV. As shown in Fig. 1B, MIA PaCa-2 and Suit2 cells are highly permissive to VSV, illustrated by high levels of VSV replication at 8 h p.i., and HPAF-II and Hs766T cells are resistant, with HPAF-II cells showing the highest level of resistance (Fig. 1B). This result is in agreement with data from our

previous studies demonstrating that VSV-resistant PDAC cell lines (such as HPAF-II and Hs766T) have upregulated type I IFN signaling and constitutive expression of a subset of ISGs, whereas VSV-permissive PDAC cell lines (such as MIA PaCa-2 and Suit2) do not (26–29). Interestingly, even though Hs766T cells had a level of VSV attachment similar to that in MIA PaCa-2 cells and even higher than that in Suit2 cells (about 3.5-fold higher based on serial dilution of the virus) (Fig. 1B), Hs766T cells showed dramatically lower levels of VSV replication than did both MIA PaCa-2 and Suit2 cells. This result suggests that the Hs766T line is not defective in VSV attachment. In contrast, HPAF-II cells showed not only the lowest levels of VSV replication but also the lowest levels of VSV attachment, suggesting that impaired VSV attachment contributes to the resistance of HPAF-II cells to VSV.

Levels of LDLR expression and LDL uptake are lower in HPAF-II cells. Recently, LDLR was proposed to be one of the receptors for VSV (16, 35, 36). As a high level of variation in LDLR expression between different cell lines of pancreatic origin was shown (37), we hypothesized that HPAF-II cells could have a defect in LDLR expression, which could explain the ineffective VSV attachment.

Three different approaches, enzyme-linked immunosorbent assays (ELISAs), Western blot analyses, and FACS analyses, were used to determine the relative levels of LDLR expression in the four PDAC cell lines. First, by using an LDLR ELISA, cell lysates were examined for cell-associated total LDLR levels in PDAC cell lines. As shown in Fig. 2A, although all four tested cell lines showed detectable levels of LDLR, the lowest level was detected in HPAF-II cells, with somewhat higher levels in MIA PaCa-2 and Suit2 cells and the highest level in Hs766T cells. When cell lysates were analyzed by Western blotting, Hs766T cells also showed the highest levels of LDLR (Fig. 2B). Interestingly, although this analysis showed similar levels of LDLR in HPAF-II, MIA PaCa-2, and Suit2 cells, HPAF-II was the only cell line with an extra band underneath the main LDLR band (Fig. 2B). This band generally represents an unglycosylated inactive form of LDLR and is often indicative of abnormal LDLR processing in cells (38–40). Because only cell surface LDLR could be utilized by the virus for attachment, LDLR cell surface expression was examined by FACS analysis using a primary antibody against LDLR. Again, EDTA, rather than trypsin, was used to retain LDLR on the cell surface. Importantly, cells were not fixed or permeabilized and were incubated at 4°C during the entire procedure to ensure that only cell surface LDLR expression was detected. As shown in Fig. 2C, although all 4 cell lines expressed LDLR at the cell surface, the lowest levels (percentage of LDLR-positive cells as well as MFI) were detected in HPAF-II cells. This could be due to HPAF-II cells expressing the unglycosylated inactive form of LDLR (Fig. 2B) that is not expressed on the cell surface (38–40).

Next, we wanted to examine LDLR functionality, which is normally done by examining the uptake of LDL, the ligand of LDLR. Importantly, LDL was previously shown to compete with VSV for LDLR (16). Therefore, the ability of LDLR to take up LDL could be used to examine LDLR functionality not only as an LDL receptor but also as a VSV receptor. To assay for LDLR functionality, PDAC cell lines were compared for their abilities to take up exogenous fluorescently labeled LDL. PDAC cells were incubated with DiI-LDL (3,3′-dioctadecylindocarbocyanine-LDL) for 4 h and then analyzed for the levels of internalized LDL by FACS analysis. As shown in Fig. 2D, LDL uptake was dramatically lower (percentage of LDL-positive cells as well as MFI) in HPAF-II cells than in all other tested cell lines. These data demonstrate that LDLR is dysfunctional in HPAF-II cells, which could lead to a defect of this cell line in VSV attachment.

PDAC cell lines express wild-type LDLR. Currently, more than a thousand different types of mutations have been found in the LDLR protein (41). Many damaging LDLR mutations affect LDLR total expression levels, maturation, surface localization, and LDL uptake (41). If present, such mutations could be responsible for the observed lower levels of LDLR expression, LDL uptake, and/or VSV attachment in HPAF-II cells. To directly examine this possibility, total RNA was isolated from HPAF-II, Hs766T, MIA PaCa-2, and Suit2 cells; cDNA was synthesized and PCR amplified by using five pairs of

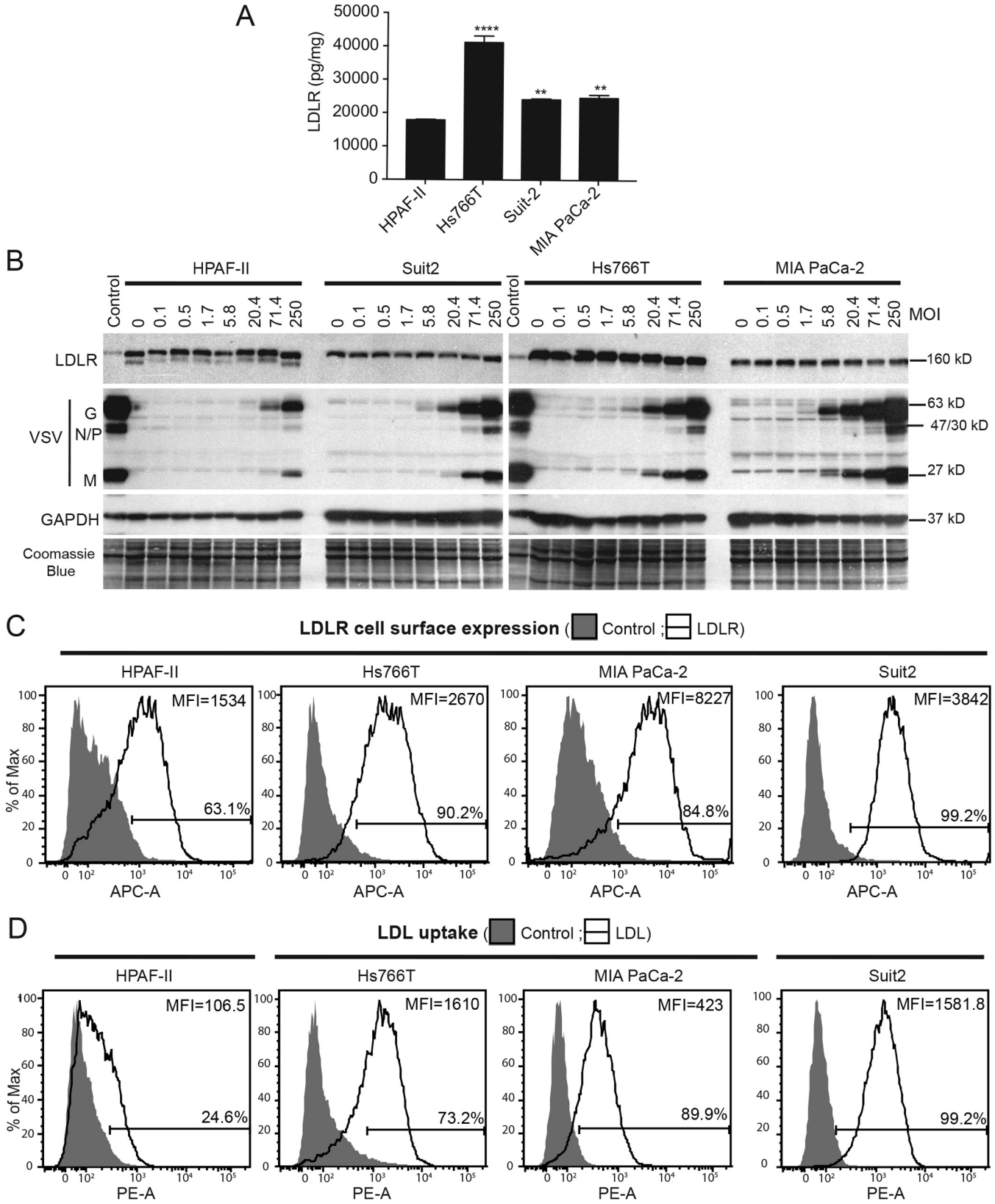

FIG 2 LDLR expression and functionality in PDAC cell lines. (A) Total protein lysates were isolated from untreated cells and analyzed for LDLR levels by an ELISA. LDLR levels were normalized to total protein levels. The assay was done in triplicate, and data represent the means ± standard errors of the means. Cell lines were compared by using 1-way analysis of variance followed by the Dunnett posttest for comparison to HPAF-II cells. **, $P < 0.01$; ****, $P < 0.0001$. (B) Cell monolayers were incubated with various amounts of VSV-ΔM51-eqFP650 (the indicated MOIs are based on virus titration on MIA PaCa-2) for 1 h at 4°C. Protein lysates were analyzed for LDLR and VSV proteins by Western blotting. Protein product sizes (kilodaltons) are indicated on the right. GAPDH and Coomassie blue

(Continued on next page)

LDLR-specific primers (42); and the overlapping PCR products, covering the entire LDLR ORF, were sequenced. Although several silent mutations were detected, sequence analysis did not detect a single mutation affecting the LDLR amino acid sequence in HPAF-II cells or any other tested PDAC cell line (data not shown). Therefore, all tested PDAC cell lines produce WT LDLR. In addition, PCR fragments were analyzed by high-resolution gel electrophoresis to detect alternatively spliced variants of LDLR, exactly as previously described (42). We did not observe any unusual PCR products, which would suggest the presence of alternatively spliced variants of LDLR in HPAF-II cells (data not shown). Together, our data show that the lower levels of LDLR expression and LDL uptake in HPAF-II cells were not due to LDLR mutations.

LDLR upregulation does not improve LDL uptake or VSV attachment in HPAF-II cells. The ELISAs (Fig. 2A), Western blot analyses (Fig. 2B), and FACS analyses (Fig. 2C) suggested potential abnormalities in the level of LDLR expression, which could explain the lower levels of LDL uptake and VSV attachment. Here we wanted to examine whether the upregulation of LDLR expression would improve LDL uptake and/or VSV attachment in HPAF-II cells.

Two different drug types were tested to increase LDLR expression levels, statins and a proprotein convertase subtilisin/kexin type 9 (PCSK9) inhibitor. Statins are competitive inhibitors of hydroxymethylglutaryl coenzyme A (HMG-CoA) reductase, which is the key rate-limiting enzyme of cholesterol synthesis. Statins inhibit cholesterol synthesis in the liver and some other cell types, including cancer cells (43). One consequence of decreased cholesterol production is that cells compensate for it by upregulating the expression of LDLR to increase cholesterol uptake from the medium (44). PCSK9 is a secretory serine protease that binds surface LDLR and induces its internalization and lysosomal degradation, thus inhibiting LDLR recycling to the surface (45). PCSK9 inhibitors bind to PCSK9 and increase LDLR cycling, thus increasing surface LDLR levels and improving LDL uptake (45). Therefore, we decided to use various statins and a PCSK9 inhibitor to increase LDLR expression and test whether this approach could improve LDL uptake and/or VSV attachment in HPAF-II cells.

To increase LDLR levels prior to the VSV attachment assay, HPAF-II cells were pretreated for 24 h with 4 widely used FDA-approved statins, atorvastatin (Lipitor), rosuvastatin (Crestor), simvastatin (Zocor), and fluvastatin (Lescol), or with a PCSK9 antagonist, SBC-110576 (46). Other tested conditions were cell starvation (0% fetal bovine serum [FBS] medium), which could increase LDLR levels (47), and the addition of unlabeled LDL, which could decrease LDLR levels (48–50). After 24 h of treatment, cell monolayers were incubated with VSV for 1 h at 4°C to examine VSV attachment by using Western blotting. As shown in Fig. 3A, LDLR expression (including the upper mature LDLR band) was strongly improved by each of the tested statins; however, VSV attachment levels were not improved. SBC-110576 and the addition of LDL did not have an effect on LDLR expression (the upper mature LDLR band) or VSV attachment. However, disappearance of the lower LDLR band was observed after SBC-110576 treatment, suggesting an expected improvement in LDLR maturation (Fig. 3A). Interestingly, starvation improved VSV attachment; however, this was likely not due to LDLR, as LDLR levels were not affected by starvation (Fig. 3A). Overall, our data demonstrate that increasing LDLR expression does not improve VSV attachment in HPAF-II cells, suggesting that lower LDLR expression levels were not a main factor in determining inefficient VSV attachment to HPAF-II cells.

FIG 2 Legend (Continued)
stain were used to confirm equal loading. (C) For LDLR cell surface expression, cells were kept on ice and were not permeabilized or fixed. After incubation with anti-LDLR primary antibody and APC-conjugated secondary antibody, cells were analyzed by FACS analysis using the APC-A channel. Control indicates cells that were incubated with secondary antibody only. "LDLR" cells were incubated with primary and secondary antibodies. Gated populations are positive for LDLR (the percentage of LDLR-positive cells is indicated above the gate line). The MFI for each population was calculated by using FlowJo software (TreeStar). Data are representative of results from 3 independent experiments. (D) For the LDL uptake assay, cells were incubated with fluorescently labeled LDL for 4 h and then analyzed by FACS analysis using the R-phycoerythrin (PE-A) channel. "Control," fluorescently labeled LDL was not added; "LDL," fluorescently labeled LDL was added. Gated populations are positive for LDL uptake (the percentage of LDL-positive cells is indicated above the gate line). The MFI for each population was calculated by using FlowJo software (TreeStar). Data are representative of results from 3 independent experiments.

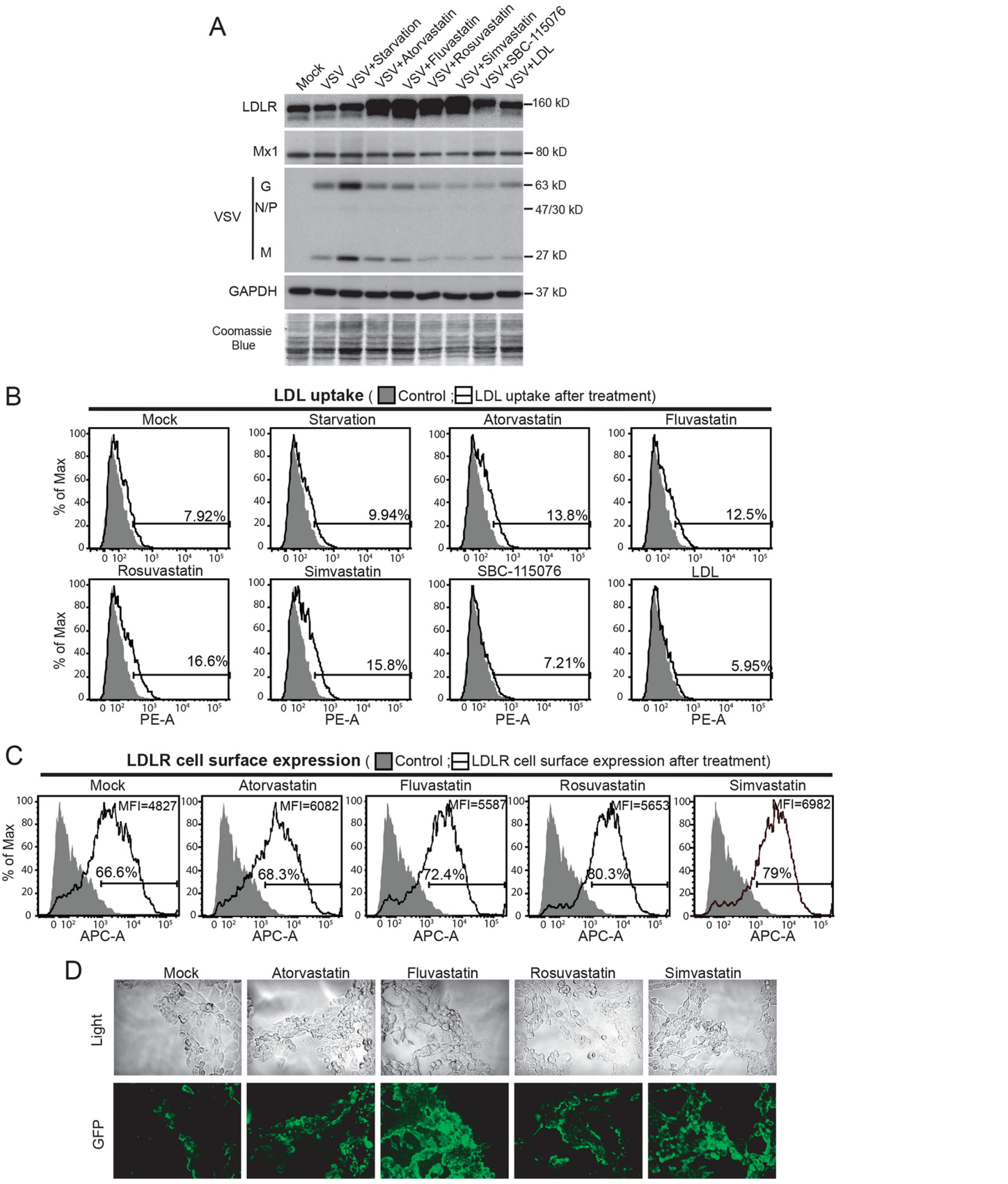

FIG 3 Effects of statins on LDLR expression, LDL uptake, and VSV attachment. (A) Cells were pretreated with statins (10 μM), SBC-115076 (10 μM), LDLR (25 μg/ml), or ruxolitinib (2.5 μM) for 24 h and then incubated with VSV-ΔM51-eqFP650 for 1 h at 4°C. The

(Continued on next page)

As VSV attachment was not improved by statins, we examined if the statin-mediated increase in LDLR expression could improve LDL uptake in HPAF-II cells. Cells were pretreated with the same statins as the ones described above for 24 h, incubated with LDL for 4 h, and analyzed by FACS analysis. Our data show only a marginal increase in LDL uptake after statin treatment (Fig. 3B). As both VSV attachment and LDL uptake were not improved by statins, we wanted to confirm that statins improve LDLR cell surface expression. HPAF-II cells were pretreated with the same statins as those used in the above-described two experiments for 24 h (Fig. 3A and B) and analyzed for surface LDLR levels by using EDTA-isolated suspension cells and FACS analysis or by analyzing HPAF-II monolayers using immunofluorescence. Cells were not fixed or permeabilized and were incubated at 4°C during the entire procedure to ensure that only cell surface LDLR expression was detected. FACS data (Fig. 3C) show that all statins improved LDLR cell surface expression (percentage of LDLR-positive cells as well as MFI). The immunofluorescence data (Fig. 3D) were in agreement with the FACS data and also showed an increase in LDLR cell surface expression. Taken together, our data indicate that the lower level of expression is not the main factor in LDLR dysfunctionality in HPAF-II cells and that some other mechanisms are responsible for inefficient LDL uptake and VSV attachment.

Role of type I IFN signaling in LDLR expression and secretion in PDAC cells. Our previous studies demonstrated that upregulated type I IFN signaling plays an important role in the resistance of PDAC cell lines to VSV (26–29) and that treatment of resistant PDAC cell lines with ruxolitinib (a specific JAK1/2 inhibitor) dramatically inhibits antiviral signaling and improves VSV replication in all resistant PDAC cell lines (28, 29). To examine whether the observed inefficient binding of VSV to HPAF-II cells is a result of type I IFN pathway upregulation, HPAF-II and Suit2 (as a negative control) cells were pretreated with ruxolitinib for 24 h before VSV attachment to cell monolayers was assayed. In agreement with data from our previous studies (28, 29), ruxolitinib treatment downregulated the ISG Mx1 in HPAF-II cells (Fig. 4A). However, treatment did not improve VSV attachment (Fig. 4A). This suggests that the defect of HPAF-II cells in VSV attachment is type I IFN independent and that inefficient attachment and upregulated antiviral signaling independently contribute to the resistance of HPAF-II cells to VSV. In agreement with this, another resistant PDAC cell line, Hs766T, does not display a defect in VSV attachment, although it has the same upregulation of type I IFN signaling as the HPAF-II cell line (26–29).

Previous studies have shown that soluble LDLR (sLDLR) secretion by cells can be induced by type I IFN and that sLDLR can inhibit VSV infection in WISH cells (this cell line was recently shown to be misidentified and identical to HeLa cells) (51–53). Although this mechanism cannot be responsible for the inefficient attachment of VSV to HPAF-II cells in our monolayer and suspension attachment assays (cells were washed before incubation with VSV), this sLDLR-mediated inhibition of VSV attachment could happen during multistep infection of cells, where HPAF-II cells show very strong resistance to VSV infection and replication. Also, previous studies have shown that

FIG 3 Legend (Continued)
MOI was 250 based on titration on MIA PaCa-2 cells. Protein isolates were used for Western blot analyses. Protein product sizes (kilodaltons) are indicated on the right. GAPDH and Coomassie blue stain were used to indicate equal loading. (B) Cells were pretreated with statins or under other conditions at the same concentrations as those described above for 24 h and then incubated with fluorescently labeled LDL for 4 h at 37°C. Samples were analyzed by FACS analysis using the PE-A channel. "Control," fluorescently labeled LDL was not added; "LDL," fluorescently labeled LDL was added. Treatments are indicated at the top of each histogram. Gated populations are positive for LDL uptake (the percentage of LDL-positive cells is indicated above the gate line). The MFI for each population was calculated by using FlowJo software (TreeStar). (C) Cells were pretreated with statins at the same concentrations as the ones described above for 24 h and then analyzed for LDLR cell surface expression. Cells were kept on ice and were not permeabilized or fixed. After incubation with anti-LDLR primary antibody and APC-conjugated secondary antibody, cells were analyzed by FACS analysis using the APC-A channel. Control indicates cells that were incubated with secondary antibody only. LDLR indicates cells that were incubated with primary and secondary antibodies. Gated populations are positive for LDLR (the percentage of LDLR-positive cells is indicated above the gate line). The MFI for each population was calculated by using FlowJo software (TreeStar). (D) Cells were pretreated with statins at the same concentrations as the ones described above for 24 h and then analyzed for LDLR cell surface expression. Cells were kept on ice and were not permeabilized or fixed. After incubation with anti-LDLR primary antibody and Alexa Fluor 488-conjugated secondary antibody, cells were observed by microscopy, and pictures were taken.

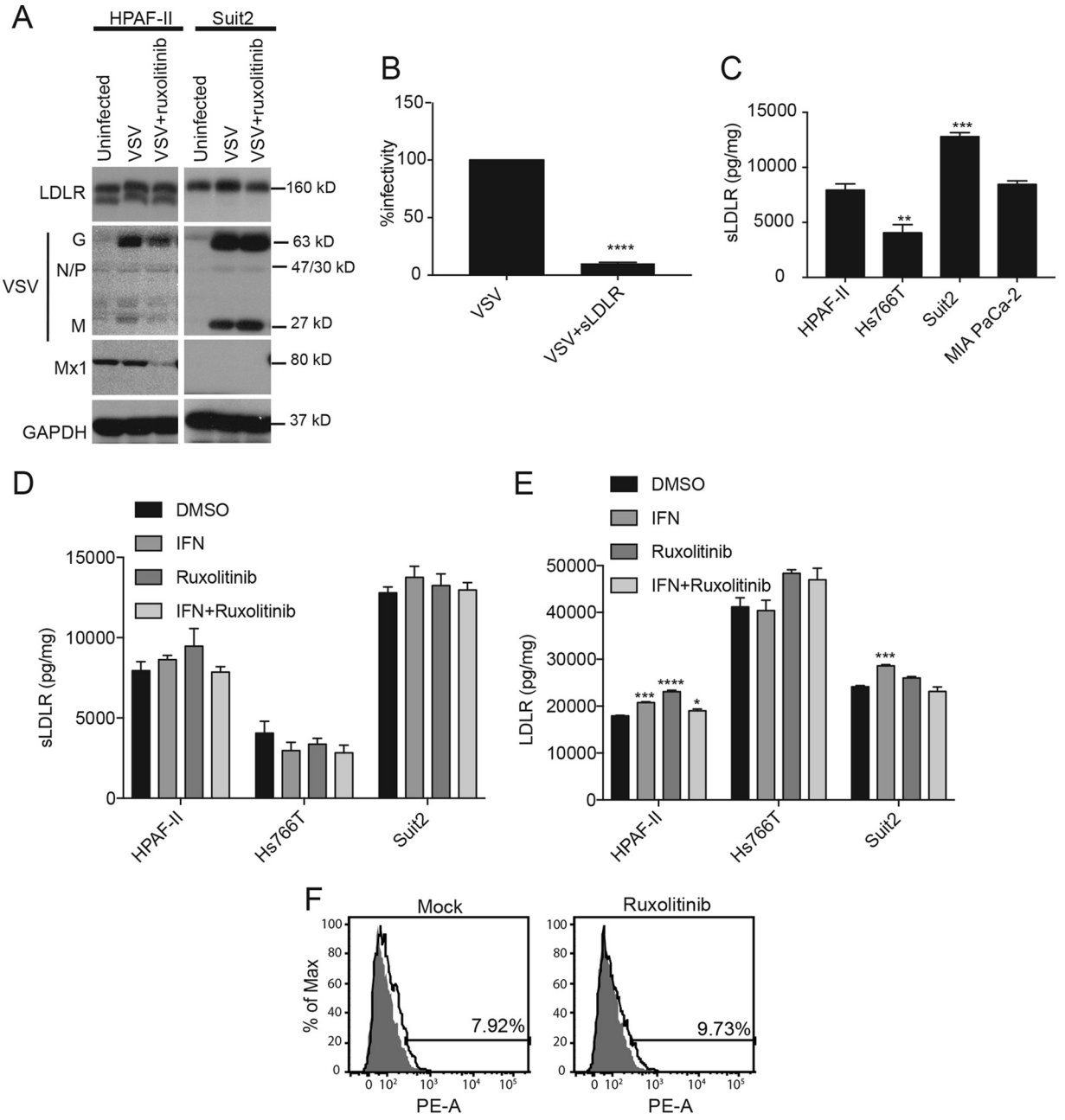

FIG 4 Effects of type I interferon and sLDLR on VSV attachment. (A) Cells were pretreated with ruxolitinib (2.5 μM) for 24 h and then incubated with VSV-ΔM51-eqFP650 (MOI of 20 based on titration on MIA PaCa-2 cells) for 1 h at 4°C. Protein was isolated and analyzed by Western blotting. Protein product sizes (kilodaltons) are indicated on the right. GAPDH was used to indicate equal loading. (B) VSV-ΔM51-eqFP650 alone or VSV-ΔM51-eqFP650 with soluble LDLR (1 μg/ml) was added to PDAC cells, and plaques were counted the next day to determine effects on infectivity. Data are representative of results from 3 independent experiments and show the means ± standard errors of the means. Conditions were compared by using an unpaired *t* test. ****, $P < 0.0001$. (C) Cells were grown in culture for 24 h, and media were then used to determine sLDLR levels by an ELISA. Soluble LDLR levels were normalized to total protein levels. The assay was done in triplicate, and data represent the means ± standard errors of the means. Conditions were compared by using 1-way analysis of variance followed by the Dunnett posttest for comparison to HPAF-II cells. **, $P < 0.01$; ***, $P < 0.001$. (D and E) Cells were treated with IFN (5,000 U/ml), ruxolitinib (2.5 μM), or IFN (5,000 U/ml)-ruxolitinib (2.5 μM) for 24 h. Medium or protein isolates were then used to determine the effect on sLDLR or LDLR levels by an ELISA. LDLR and sLDLR levels were normalized to total protein levels. The assay was done in triplicate, and data represent the means ± standard errors of the means. Conditions were compared by using 1-way analysis of variance followed by the Dunnett posttest for comparison to the control. *, $P < 0.05$; ***, $P < 0.001$; ****, $P < 0.0001$. (F) Cells were pretreated with ruxolitinib (2.5 μM) for 24 h and then incubated with fluorescently labeled LDL for 4 h at 37°C. Samples were analyzed by FACS analysis using the PE-A channel. "Control," fluorescently labeled LDL was not added; "LDL," fluorescently labeled LDL was added. Treatments are indicated at the top of each histogram. The "mock" sample is the same as the one in Fig. 3B. Gated populations are positive for LDL uptake (the percentage of LDL-positive cells is indicated above the gate line). The MFI for each population was calculated by using FlowJo software (TreeStar).

O-glycosylation in the stem region of LDLR is important for the cell surface expression and stability of this receptor and that the absence of such *O*-glycosylation can lead to proteolytic cleavage and the release of the bulk of the N-terminal extracellular domain of the receptor into the medium (54, 55). Therefore, an extensive release of sLDLR into the medium could be indicative of abnormal LDLR *O*-glycosylation in HPAF-II cells.

First, to test whether sLDLR can inhibit VSV infectivity in PDAC cells, sLDLR and VSV or VSV alone was added to the cells, and the cells were incubated for 30 min at 37°C (the assay was conducted as described previously [51–53]). Cells were then washed to remove any unbound virus and overlaid with agar to prevent secondary infections. VSV plaques were counted to determine the effect of sLDLR on VSV infectivity. As shown in Fig. 4B, the presence of exogenous sLDLR led to a 10-fold decrease in VSV infectivity, confirming that sLDLR secretion could potentially inhibit VSV attachment in PDAC cell lines. To examine the levels of secreted sLDLR produced by different PDAC cell lines, cells were incubated in medium without FBS for 24 h, and the medium was then collected and analyzed for sLDLR by an ELISA. As shown in Fig. 4C, the tested PDAC cell lines produced different amounts of sLDLR. Importantly, HPAF-II cells did not produce the most sLDLR, possibly suggesting that there are no abnormalities in this cell line in *O*-glycosylation or other mechanisms associated with the excessive secretion of sLDLR.

In addition, the effects of type I IFN on sLDLR secretion or total LDLR levels in PDAC cells were examined. PDAC cell lines were treated with either IFN-α (to stimulate type I IFN signaling), ruxolitinib (to inhibit it), or both, and sLDLR (Fig. 4D) and cell-associated LDLR (Fig. 4E) levels were analyzed by using an ELISA. In contrast to previous studies with WISH cells (51, 52), these treatments had either no or negligible effects on sLDLR production and cell-associated LDLR. Furthermore, when HPAF-II cells were treated with ruxolitinib (to inhibit type I IFN signaling), LDL uptake was not improved (Fig. 4F). Together, our data demonstrate that HPAF-II cells do not display abnormalities in sLDLR secretion levels and that LDLR expression, LDL uptake, and VSV attachment in PDAC cells are controlled independently of type I IFN signaling.

Polycations improve VSV attachment to HPAF-II cells. Our data show that inefficient VSV attachment to HPAF-II cells, as well as defective LDL uptake, could not be improved in HPAF-II cells even when LDLR expression was markedly increased by treating cells with statins (Fig. 3). While future studies are needed to identify specific defects of LDLR in LDL uptake and VSV attachment, here we decided to use an alternative approach to improve VSV attachment by targeting LDLR-independent VSV attachment. Previous studies suggested that phosphatidylserine (17–19), sialoglycolipids (20), heparan sulfate (21), or electrostatic interactions between VSV and the cell membrane (56, 57) could play an important role in VSV attachment. As none of those studies examined PDAC cell lines, we wanted to confirm that LDLR-independent attachment also occurs in PDAC cell lines. Cells were treated with 0.2% EDTA (control) or 0.05% trypsin in phosphate-buffered saline (PBS) for 30 min at 37°C to digest surface LDLR and then used for FACS analysis of VSV attachment to cells in suspension (Fig. 5A). To confirm the successful digestion of LDLR by trypsin, total protein was isolated from trypsin-treated cells and analyzed by Western blotting for LDLR (Fig. 5B). Despite the lack of any detectable LDLR in trypsin-treated HPAF-II, MIA PaCa-2, and Suit2 cell lines and the significant decrease in the level of mature LDLR (upper band) in Hs766T cells (Fig. 5B), VSV attachment occurred in all cell lines (Fig. 5A). Again, HPAF-II cells showed the lowest level of VSV attachment, as they are defective in VSV attachment, even in the presence of LDLR, when the analyzed cells were detached by using EDTA (Fig. 5A). These data suggest that VSV particles can attach to PDAC cells in an LDLR-independent manner.

There are several approaches to improve LDLR-independent VSV attachment to cells. Several early studies demonstrated that different pH conditions or the addition of positively charged polycations, such as Polybrene or DEAE-dextran, can significantly improve VSV attachment to various cell membrane components via nonspecific electrostatic interactions (56–58). Moreover, Polybrene and other polycations are routinely

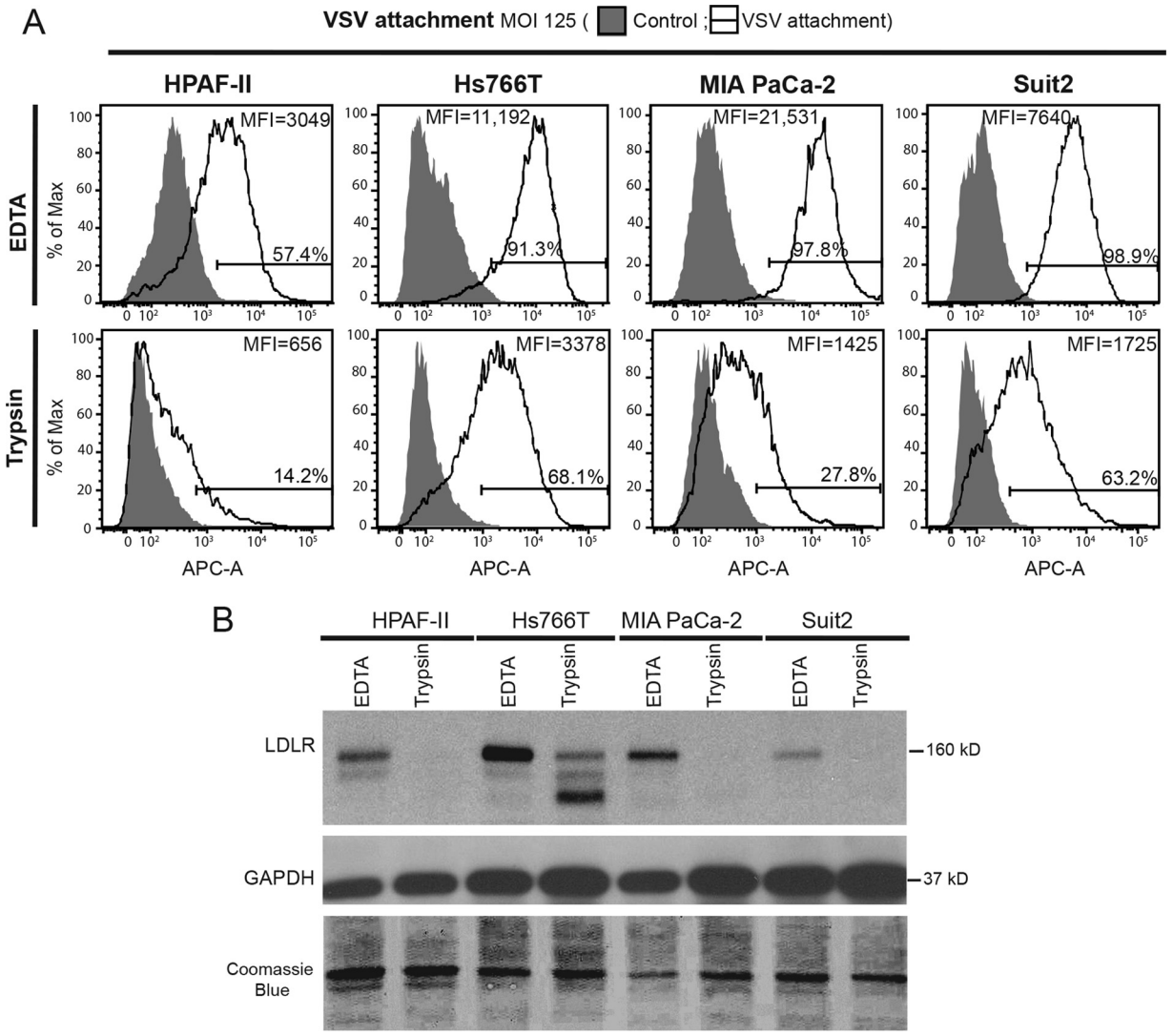

FIG 5 Effect of LDLR digestion by trypsin on VSV attachment. Cells were treated with PBS with 0.2% or 0.05% trypsin and then used for VSV-ΔM51-eqFP650 attachment analysis, or protein was isolated to confirm LDLR digestion. (A) For the attachment assay, after a 1-h incubation with VSV-ΔM51-eqFP650 (MOI of 125 based on titration on MIA PaC-2 cells) at 4°C, cells were incubated with anti-VSV-G antibody and APC-conjugated secondary antibody and analyzed by FACS analysis using the APC-A channel. Control cells were mock treated (without VSV-ΔM51-eqFP650), and primary and secondary antibodies were used. "VSV attachment" cells were incubated with VSV-ΔM51-eqFP650. Gated populations are positive for VSV attachment (the percentage of VSV-positive cells is indicated above the gate line). The MFI for each population was calculated by using FlowJo software (TreeStar). (B) Protein was isolated and analyzed by Western blotting. Protein product sizes (kilodaltons) are indicated on the right. GAPDH and Coomassie blue stain were used to indicate equal loading.

used to improve the transduction of target cells with replication-defective lentiviral particles that are pseudotyped with VSV-G (59–61). Therefore, all these conditions were examined to identify a way to improve VSV attachment to HPAF-II cells. Our original screen was conducted under the most optimal conditions for VSV attachment, and we used VSV-driven GFP expression as a readout of virus infection/replication. Any conditions stimulating VSV infection were then studied in subsequent experiments for their specific effect on VSV attachment. To examine whether pH or polycations can improve VSV infection of HPAF-II cells, cells were pretreated with various concentrations of protons (pH levels), Polybrene, or DEAE-dextran for 30 min and then incubated with VSV for 1 h at 37°C under each test condition (Fig. 6A and B). Virus and chemical reagents were then removed, cells were placed back at 37°C for 46 h, and VSV infection-driven GFP fluorescence was measured. As different pH conditions or polycations were present for only 1 h 30 min and removed after virus incubation, the differences in VSV-associated GFP fluorescence identified in this original screening likely

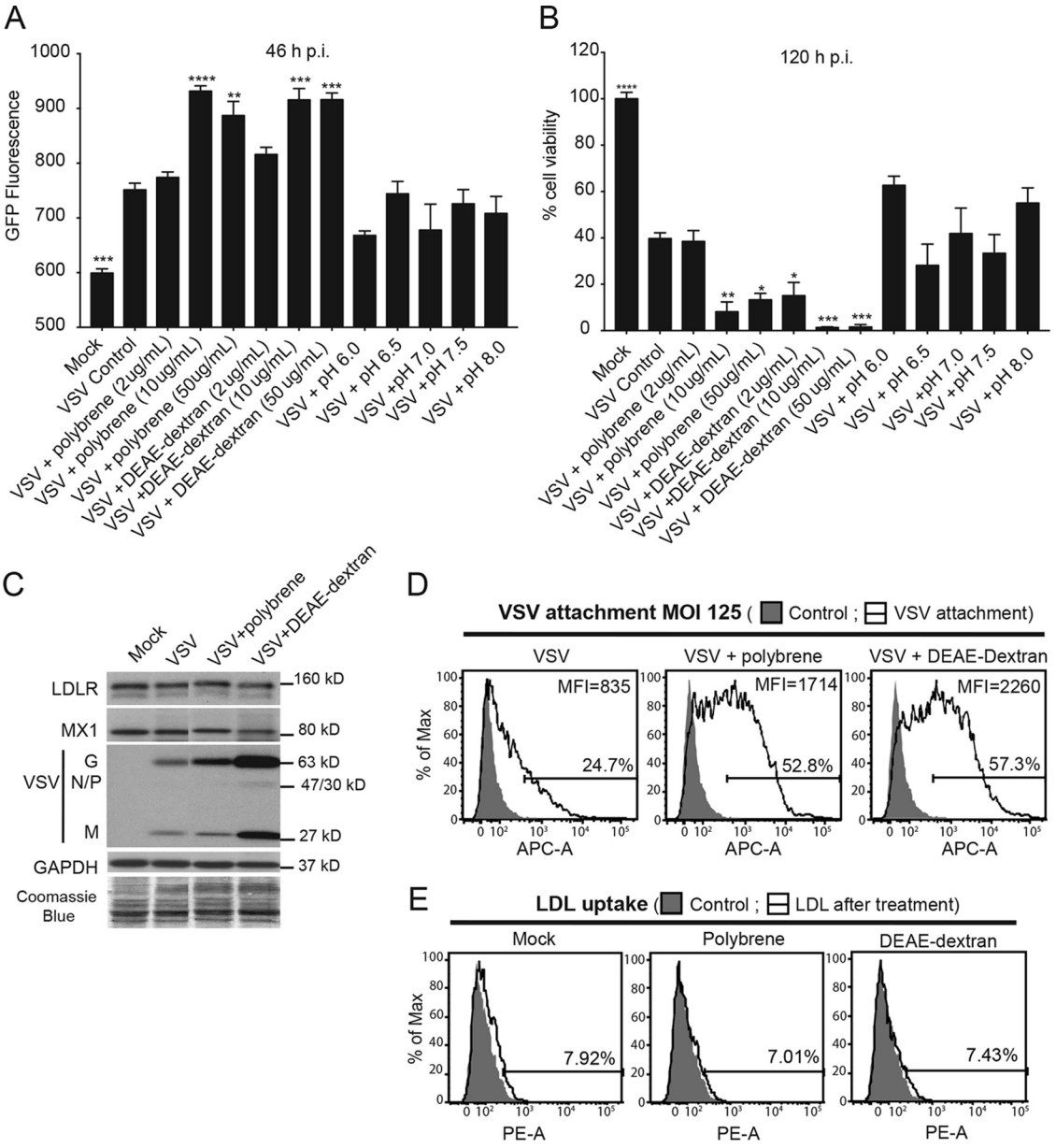

FIG 6 Effects of polycation treatment on VSV attachment, replication, and oncolysis. (A and B) Cells were treated with MEM (without FBS) containing Polybrene, DEAE-dextran, or a different pH for 30 min, and then VSV-ΔM51-GFP at an MOI of 0.1 (based on titration on HPAF-II cells) was added for 1 h at 37°C (under the same conditions). Cells were then washed and incubated at 37°C. (A) GFP fluorescence was analyzed at 46 h p.i. The assay was done in triplicate, and data represent the means ± standard errors of the means. Conditions were compared by using 1-way analysis of variance followed by the Dunnett posttest for comparison to "+VSV Control." *, $P < 0.05$; **, $P < 0.01$; ***, $P < 0.001$; ****, $P < 0.0001$. (B) At 5 days p.i., cells were analyzed for viability by an MTT assay. The assay was done in triplicate, and data represent the means ± standard errors of the means. Conditions were compared by using 1-way analysis of variance followed by the Dunnett posttest for comparison to "VSV Control" representing cells treated with VSV only. *, $P < 0.05$; **, $P < 0.01$; ***, $P < 0.001$; ****, $P < 0.0001$. (C) Cells were pretreated with Polybrene (10 μg/ml) and DEAE-dextran (10 μg/ml) and then incubated with VSV-ΔM51-eqFP650 for 1 h at 4°C. The MOI was 250 based on titration on MIA PaCa-2 cells. Protein isolates were used for Western blot analyses. Protein product sizes (kilodaltons) are indicated on the right. GAPDH and Coomassie blue stain were used to indicate equal loading. Samples were run on the same gel, and irrelevant lanes were removed. (D) Cells in suspension were treated as described above. The MOI was 125 based on titration on MIA PaCa-2 cells. After incubation with VSV-G primary antibody and APC-conjugated secondary antibody, cells were analyzed by FACS analysis using the APC-A channel. Control indicates cells that were mock treated (without VSV), and primary and secondary antibodies were used. "VSV attachment" cells were incubated with various amounts of VSV (the indicated MOIs are based on virus titration on MIA PaCa-2 cells). Gated populations are positive for VSV attachment (the percentage of VSV-positive cells is indicated above the gate line). The MFI for each population was calculated by using FlowJo software (TreeStar). (E) Cells were pretreated at the same concentrations as the ones described above and then incubated with fluorescently labeled LDL for 4 h at 37°C. Samples were analyzed by FACS analysis using the PE-A channel. "Control," fluorescently labeled LDL was not added; "LDL," fluorescently labeled LDL was added. Treatments are indicated at the top of each histogram. The mock samples are the same as the ones in Fig. 3B. Gated populations are positive for LDL uptake (the percentage of LDL-positive cells is indicated above the gate line). The MFI for each population was calculated by using FlowJo software (TreeStar).

reflected the efficacy of initial VSV infection. None of the pH conditions improved VSV infection in HPAF-II cells (Fig. 6A [GFP fluorescence under each condition is compared to GFP fluorescence in HPAF-II cells treated with VSV only]). However, under all tested conditions, the two highest concentrations tested (10 μg/ml and 50 μg/ml) of Polybrene and DEAE-dextran showed a clear increase in VSV infectivity (Fig. 6A). To examine whether the improved VSV infectivity under these treatment conditions results in increased oncolysis, a methylthiazolyldiphenyl-tetrazolium (MTT) cell viability assay was performed at 5 days p.i. Compared to VSV alone ("VSV control"), the 2 highest concentrations (10 and 50 μg/ml) of Polybrene and all 3 concentrations of DEAE-dextran significantly decreased cell viability (Fig. 6B).

To examine whether the observed improvement in VSV infectivity was due to an improvement in VSV attachment, cells in monolayers or in suspension were pretreated with 10 μg/ml of Polybrene or DEAE-dextran for 30 min and then incubated with VSV for 1 h at 4°C (to prevent virus entry) in the presence of these polycations. Cells were washed to remove any unbound virus, and protein was then isolated from cells in monolayers and analyzed by Western blotting, or cells in suspension were used for FACS analysis. Both Polybrene and DEAE-dextran treatments showed a clear improvement in VSV attachment using both methods, even though the improvement with DEAE-dextran was stronger (Fig. 6C and D). The FACS data showed that polycations more than doubled the number of cells attached by VSV (Fig. 6D).

We then tested whether the improved VSV attachment to HPAF-II cells was possibly due to increased LDLR expression or functionality as a result of treatments of cells with polycations. Pretreatment of cells with 10 μg/ml of Polybrene or DEAE-dextran for 30 min, followed by incubation with VSV for 1 h at 4°C in the presence of these polycations, did not improve LDLR expression (Fig. 6C). Furthermore, when cells were pretreated with 10 μg/ml of Polybrene or DEAE-dextran for 30 min and then incubated with LDL for 4 h at 37°C in the presence of these polycations, no improvement in LDL uptake was observed when cells were analyzed by FACS analysis (Fig. 6E). Taken together, these data indicate that Polybrene and DEAE-dextran improve VSV attachment to HPAF-II cells via an LDLR-independent mechanism.

Combining Polybrene or DEAE-dextran with ruxolitinib breaks resistance of PDAC cells to VSV. We showed previously that the treatment of HPAF-II and other resistant PDAC cell lines with JAK1/2 inhibitors significantly improved their permissiveness to VSV (27–29). However, JAK inhibitor I treatment only moderately improves the susceptibility of resistant cells to initial VSV infection (27), and pretreatment of cells with ruxolitinib (compared to posttreatment only) did not change the kinetics of VSV replication, with a significant increase in VSV replication that could be seen only after 48 h p.i., even in cells pretreated with ruxolitinib for up to 48 h, suggesting that ruxolitinib did not improve the rate of initial infection but rather facilitated secondary infection via an inhibition of antiviral signaling in PDAC cells (27–29). As Polybrene and DEAE-dextran improve VSV attachment and primary infection and ruxolitinib improves VSV replication, we hypothesized that combining these two treatments would improve overall VSV infection and oncolysis in HPAF-II cells. Cells were pretreated with 10 μg/ml Polybrene or DEAE-dextran or mock treated for 30 min; VSV was then added in the presence of polycations (or mock treatment) for 1 h at 37°C, followed by medium removal and washes with PBS; and cells were then incubated in the presence of 2.5 μM ruxolitinib or mock treatment. VSV infection-associated GFP fluorescence was monitored for 71 h. In agreement with data from our previous study (28), ruxolitinib alone significantly improved VSV replication starting at 48 h p.i.; however, the polycation-ruxolitinib combinations showed an even stronger improvement (Fig. 7A). Importantly, not only did the polycation-ruxolitinib combinations result in higher-level VSV replication (Fig. 7A), but also a significant increase in VSV replication was already seen at 24 h p.i. versus that at 48 h p.i. for ruxolitinib treatment only (Fig. 7A), which is likely due to Polybrene and DEAE-dextran improving the rate of initial infections, as these polycations were present only during 1 h of incubation of HPAF-II cells with VSV. Figure 7B shows representative pictures of the treated cells at 22 and 48 h p.i., and it confirms

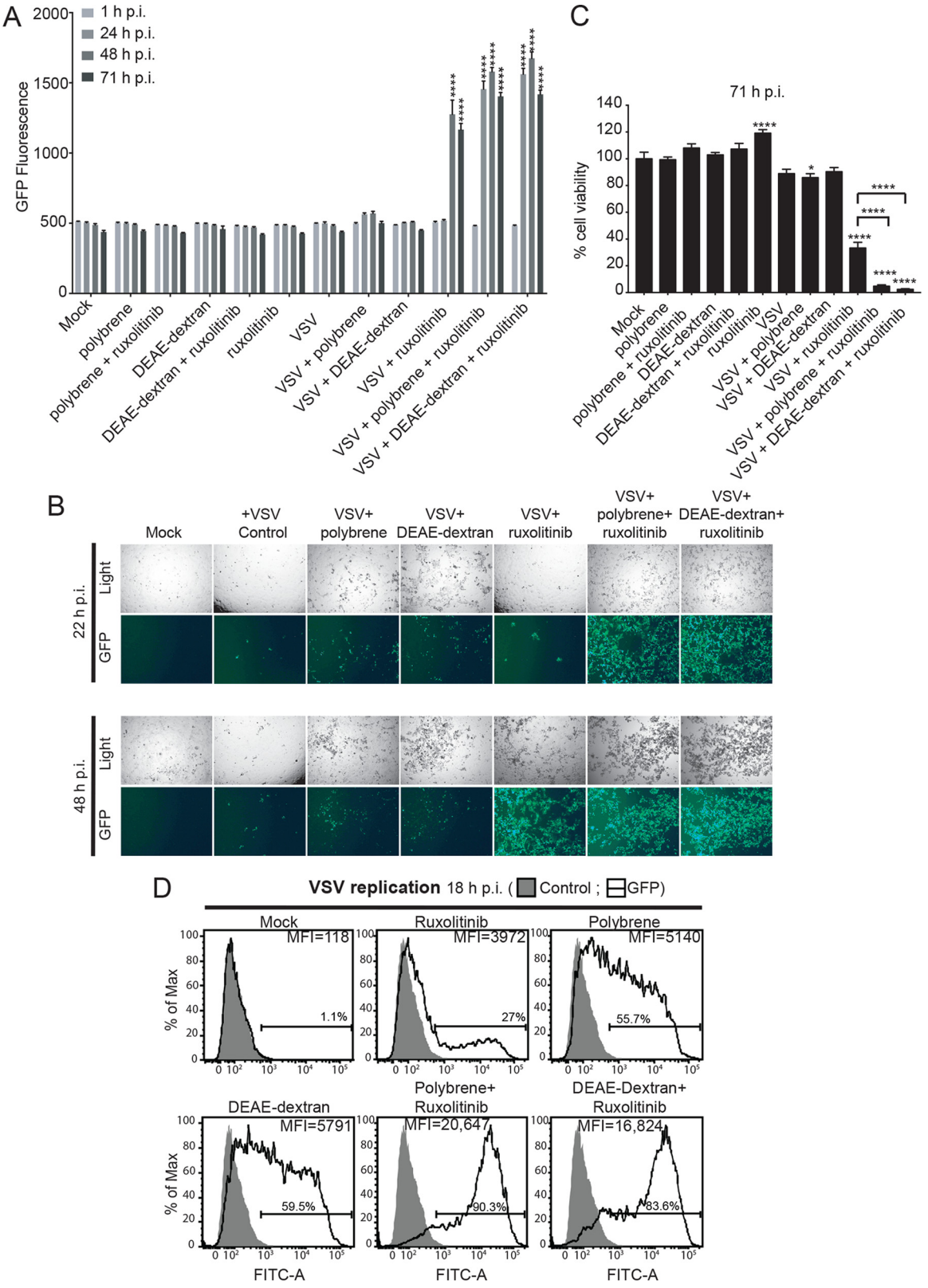

FIG 7 Effects of combining polycations with ruxolitinib on VSV infection and oncolysis in HPAF-II cells. Cells were pretreated with 10 μg/ml Polybrene or DEAE-dextran or mock treated for 30 min, and VSV-ΔM51-GFP at an MOI of 0.001 (based on titration on HPAF-II cells) was then added in the presence of polycations (or mock treated) for 1 h at 37°C, followed by medium removal, washes with PBS, and then incubation in the presence of 2.5 μM ruxolitinib or mock treatment. (A to C) VSV infection-associated GFP fluorescence was monitored for 71 h (A), pictures were taken (B), and an MTT assay was then performed to determine cell viability (C). The assay was done in triplicate, and data represent the means ± standard errors of the means. For GFP fluorescence, conditions were compared by using 2-way analysis

(Continued on next page)

that an important improvement in VSV replication can already be seen at 22 h p.i. for the polycation-ruxolitinib combinations. To examine whether the improved VSV infectivity under these treatment conditions results in increased oncolysis, an MTT cell viability assay was performed at 71 h p.i. Ruxolitinib improved oncolysis significantly; however, the polycation-ruxolitinib combination significantly improved oncolysis compared to that with treatment with ruxolitinib alone (Fig. 7C).

To confirm that Polybrene and DEAE-dextran improve initial infections, HPAF-II cells were treated as described above; however, cells were analyzed by FACS analysis for the number of infected cells at an earlier time point (18 h p.i.) when, for HPAF-II cells, we generally observe only initially infected cells (Fig. 8D). Polybrene and DEAE-dextran treatments resulted in many more GFP-positive cells (55.7% and 55.9%, respectively, versus 1.1% for VSV only) than with ruxolitinib treatment (27%), confirming that these polycations improved initial infection. When the polycations were combined with ruxolitinib, almost all cells were infected (90.3% and 83.6% for Polybrene-ruxolitinib and DEAE-dextran–ruxolitinib, respectively), likely because initial infections were improved by Polybrene or DEAE-dextran and secondary infections were improved by ruxolitinib via an enhancement of VSV replication in initially infected cells and an inhibition of antiviral responses in the secondarily infected cells. Taken together, polycations and ruxolitinib complement each other when combined and break the multiple mechanisms of resistance of HPAF-II cells to VSV.

To evaluate if the combination treatment could work on a broad spectrum of PDAC cell lines, Hs766T, MiaPaCa-2, and Suit2 cells were treated as described above for HPAF-II cells (Fig. 7A and B). The VSV-resistant PDAC cell line Hs766T and the VSV-permissive cell line Suit2 responded in a manner similar to that of HPAF-II cells, as the combination treatment resulted in higher-level VSV replication, and a significant increase in VSV replication was already seen at 22 h p.i. versus that at 46 h p.i. for ruxolitinib treatment only (Fig. 8). The VSV-permissive cell line MiaPaCa-2 also resulted in somewhat higher levels of VSV replication; however, a smaller increase was seen at 22 h p.i. than with ruxolitinib alone (Fig. 8). This is not surprising, as the MiaPaCa-2 cell line is the most permissive PDAC cell line, and based on our previous studies, it has the strongest defect in antiviral signaling (26–29). To examine whether the improved VSV infectivity under these treatment conditions results in increased oncolysis, an MTT cell viability assay was performed at 68 h p.i. Oncolysis of the VSV-resistant PDAC cell line Hs766T was significantly improved by ruxolitinib treatment; however, the polycation-ruxolitinib combination significantly improved oncolysis compared to that with ruxolitinib (Fig. 8). With VSV-mediated oncolysis already being very efficient in VSV-permissive PDAC cell lines, the polycation-ruxolitinib combination did not improve oncolysis (Fig. 8). Taken together, polycations and ruxolitinib can improve VSV treatment outcomes in a wide spectrum of PDAC cell lines.

DISCUSSION

In this study, we examined the possible role of virus attachment in the resistance of some human PDAC cell lines to VSV, as it is the first critical stage for successful viral infection. We demonstrate that the HPAF-II cell line, the most resistant PDAC cell line, in addition to an upregulated type I IFN signaling and constitutive expression of ISGs, also shows impaired VSV attachment. This result was surprising, as VSV is known for its pantropism and the ability to infect virtually any cell line (of vertebrate or invertebrate origin) in the laboratory (7). Importantly, pretreatment of HPAF-II cells with ruxolitinib did not improve VSV attachment, indicating that type I IFN signaling does not play a

FIG 7 Legend (Continued)
of variance followed by the Dunnett posttest for comparison to mock treatment. ****, $P < 0.0001$. The MTT conditions were compared by using 1-way analysis of variance followed by the Dunnett posttest for comparison to mock treatment (or also VSV plus ruxolitinib for the last three conditions). *, $P < 0.05$; ***, $P < 0.001$; ****, $P < 0.0001$. (D) The percentage of GFP-positive cells was determined at 18 h p.i. by FACS analysis using the fluorescein isothiocyanate (FITC-A) channel. Gated populations are positive for GFP. "Control" represents cells alone, and "GFP" represents GFP-positive cells in which VSV replication occurred. Gated populations are positive for VSV replication. The MFI for each population was calculated by using FlowJo software (TreeStar).

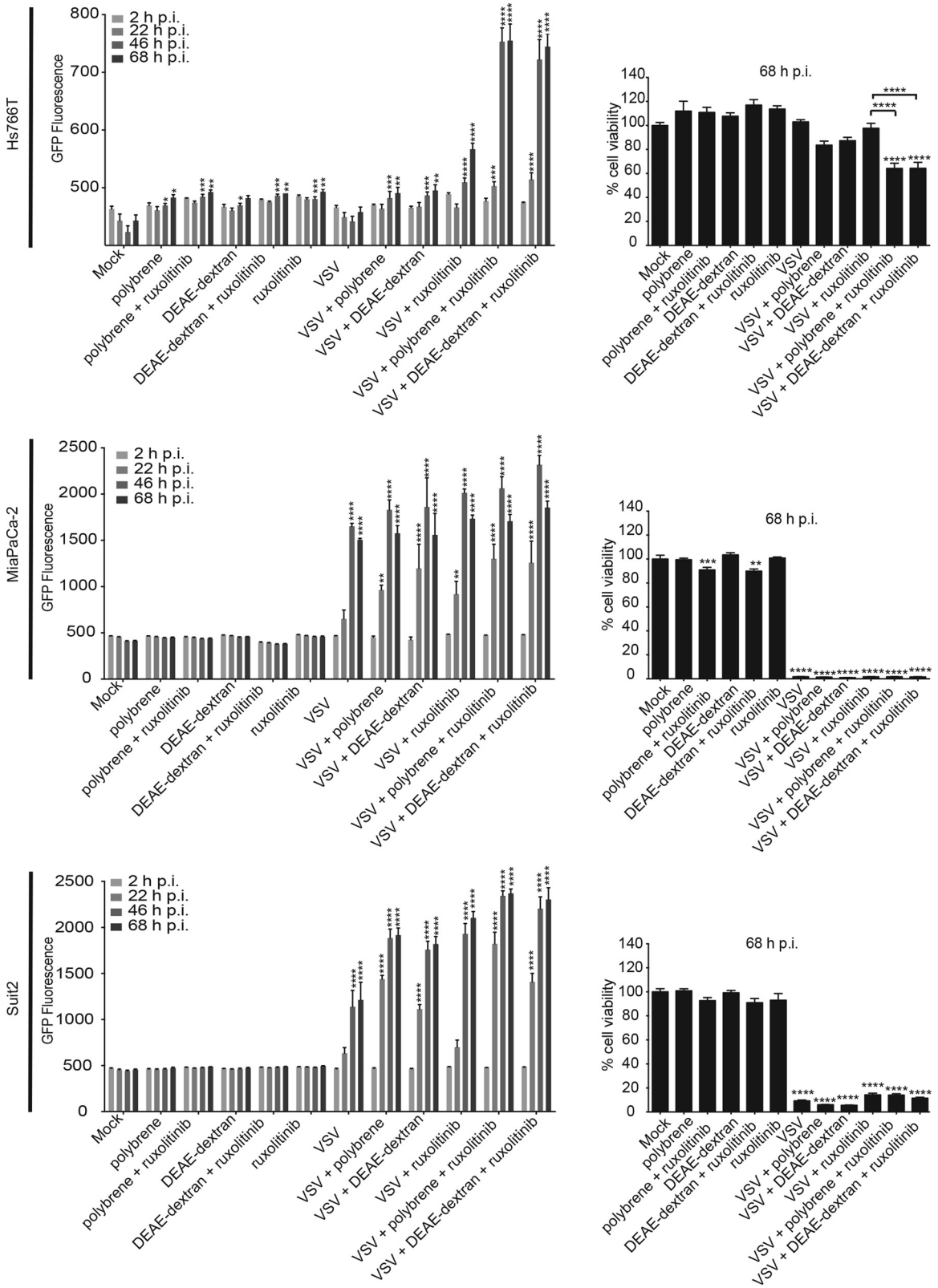

FIG 8 Effects of combining polycations with ruxolitinib on VSV infection and oncolysis in other PDAC cell lines. Cells were pretreated with 10 μg/ml Polybrene or DEAE-dextran or mock treated for 30 min, and VSV-ΔM51-GFP at an MOI of 0.001 (cell line specific) was then added in the presence of polycations (or mock treated) for 1 h at 37°C, followed by medium removal, washes with PBS, and then incubation in the presence of 2.5 μM ruxolitinib or mock treatment. VSV infection-associated GFP fluorescence was monitored for 68 h, and an MTT assay was then performed to determine cell viability. The assay was done in triplicate, and data represent the means ± standard errors of the means. For GFP fluorescence, conditions were compared by using 2-way analysis of variance followed by the Dunnett posttest for

(Continued on next page)

major role in VSV attachment. In general, our results suggest that HPAF-II cells are highly resistant to VSV because they are not only nonpermissive to VSV replication due to their constitutive antiviral state but also nonsusceptible to VSV due to impaired virus attachment, which is type I IFN independent.

As LDLR has been shown to be one of the receptors for VSV (16, 35, 36), our study examined if HPAF-II cells have a defect in LDLR expression or functionality. Our data show that HPAF-II cells have lower LDLR expression levels. Moreover, based on data from the LDL uptake assay, HPAF-II cells express dysfunctional LDLR, which could explain the defect of this cell line in VSV attachment. More than a thousand different types of mutations have been found in the LDLR protein, which affect LDLR expression or functionality (41). With mutations being so common in LDLR, we hypothesized that the HPAF-II cell line could have a mutation in LDLR, which would explain its defects in LDL uptake and VSV attachment. However, our sequence analysis of LDLR mRNA showed no mutations affecting the LDLR amino acid sequence in HPAF-II cells (or the other 3 tested PDAC cell lines), suggesting that another factor(s) is responsible for the lower expression levels and/or activities of LDLR in HPAF-II cells. To improve LDLR expression and LDL uptake, HPAF-II cells were treated with statins. Although all four tested statins strongly increased total and surface LDLR expression levels, this increase did not improve LDL uptake and VSV attachment in HPAF-II cells.

Taken together, the defective uptake of LDL and impaired VSV attachment in HPAF-II cells were not determined by mutations or relatively lower LDLR expression levels in this cell line but via some other mechanism(s). Previous studies have shown that *O*-glycosylation in the stem region of LDLR is important for the cell surface expression and stability of this receptor. The absence of *O*-glycosylation in the stem region can lead to proteolytic cleavage and the release of the bulk of the N-terminal extracellular domain of the receptor into the medium (54, 55). It is possible that HPAF-II cells lack *O*-glycosylation; however, it is important to note that HPAF-II cells did not release the most sLDLR into the medium, compared to other tested PDAC cell lines, which express functional LDLR. It has also been suggested that the N-terminal segment of LDLR also has *O*-glycans (62). Although that same study demonstrated that *O*-glycosylation at the N-terminal segment of LDLR did not affect LDLR cell surface expression and LDL binding/internalization (62), another group showed with another cell line that N-terminal *O*-glycosylation is important for LDLR function, as it showed an effect on LDL binding (63).

It is also possible that HPAF-II cells express normal levels of functional LDLR but that a negative factor on the cell surface of HPAF-II cells interferes with LDL uptake, VSV attachment, and even LDLR antibody binding in our FACS assay. Interestingly, mucin MUC1 overexpression in some PDAC cell lines, including HPAF-II, has been shown to limit the uptake of anticancer drugs by tumor cells (64, 65). It is possible that MUC1 and other mucins mask LDLR and prevent both VSV attachment and LDL uptake. Future studies will examine all these possibilities.

As the statin-mediated increase in LDLR expression did not improve VSV attachment or LDLR functionality, we evaluated LDLR-independent mechanisms to improve VSV attachment. While LDLR has been suggested to be one of the receptors for VSV (16), previous studies also suggested that phosphatidylserine (17–19), sialoglycolipids (20), heparan sulfate (21), and virus-cell membrane electrostatic interactions (56, 57) may play an important role in VSV attachment. We employed a cell surface "shaving" technique with trypsin to remove surface LDLR, and our data showed that VSV can indeed attach to PDAC cells independently of LDLR. We then decided to test two commonly used polycations, Polybrene and DEAE-dextran, which were previously shown to improve VSV attachment (56, 57) and also used in various applications using

FIG 8 Legend (Continued)
comparison to mock treatment. ****, $P < 0.0001$. The MTT conditions were compared by using 1-way analysis of variance followed by the Dunnett posttest for comparison to mock treatment (or also to VSV plus ruxolitinib for the last three conditions). *, $P < 0.05$; ***, $P < 0.001$; ****, $P < 0.0001$.

VSV-G-pseudotyped lentiviruses (59–61). The addition of these polycations strongly improved VSV attachment, VSV infection, and VSV-induced cell death. These improvements in VSV attachment were LDLR independent, as the polycations had no effect on LDL uptake or LDLR expression.

As both the cell and virus lipid membranes possess net negative charges, it has been suggested that polycations act by counteracting repulsive electrostatic effects and, thus, improving attachment. Early studies showed that treatment of HeLa cells with Polybrene has to be done before infection and/or during infection but not after infection with VSV (56, 58). Those studies concluded that Polybrene must have an effect on VSV binding to cells, potentially by improving virus-receptor interactions. Previous studies on DEAE-dextran made similar observations and concluded that alterations in the cell surface charge distribution enhance VSV attachment (56, 57). More recent studies using retroviruses reported that Polybrene increased their attachment by 10-fold (66). Interestingly, this enhancement was receptor and virus envelope independent, as retrovirus adsorption occurred equivalently on receptor-positive and -negative cells as well as with envelope-positive and -negative ("bald") virus particles. That study concluded that electrostatic interactions play an important role in mediating early virus-cell interactions (66).

Not only do our data show that polycations strongly improve VSV attachment to HPAF-II cells, but we also successfully used a novel triple-combination treatment to break multiple mechanisms of resistance of HPAF-II cells to VSV. We have previously shown that pretreatment of cells with ruxolitinib (compared to posttreatment only) did not change the kinetics of VSV replication, suggesting that ruxolitinib had a modest effect on initial infection but mainly facilitated secondary infection via inhibition of antiviral signaling in PDAC cells (28, 29). Here, combining polycations (to improve initial infection) with ruxolitinib (to improve viral replication) not only improved overall VSV replication and oncolysis but also accelerated VSV replication kinetics by 24 h compared to treatment with ruxolitinib only (Fig. 9).

The primary goal of this study was to determine if VSV attachment could be a limiting factor in VSV-based oncolytic virotherapy against PDAC. We demonstrated that VSV attaches significantly less to the most resistant PDAC cell line HPAF-II, and this mechanism contributes to the resistance of HPAF-II cells to VSV infection. Also, for the first time, we show that combining a polycation with a JAK inhibitor can improve the outcome of oncolytic virus treatment *in vitro*. Future experiments will test at least some of these combinations *in vivo* in a clinically relevant PDAC animal model. Previous studies examining polycations were done in the context of gene therapy to improve viral as well as nonviral gene delivery (67), as inefficient gene delivery is often a major limitation in the success of gene therapy (68). The effects of polycations *in vitro* and *in vivo* have been extensively studied for adenovirus-based gene therapy vectors. Several studies in different mouse models have shown that combining adenovirus with different polycations (including DEAE-dextran) can improve adenovirus-mediated gene transfer without any additional toxicity (69–72). As polycations improve adenovirus-mediated gene transfer, less virus would have to be used, which would improve the therapeutic index by reducing unwanted responses associated with high doses of virus. On the other hand, multiple reports indicate that polycations could exhibit nonspecific cytotoxicity *in vivo* as well as *in vitro* (73, 74), with some studies demonstrating unacceptable cytotoxicity for DEAE-dextran (74, 75) and Polybrene (76, 77), at least under some experimental conditions. Therefore, while our study conceptually demonstrates the feasibility of the polycation-mediated improvement of VSV-based OV therapy *in vitro*, future studies are needed to compare Polybrene and DEAE-dextran to other polycations that could be used safely and effectively *in vivo* in combination with VSV and ruxolitinib. For instance, the nonspecific cytotoxicity of polycations is already being addressed currently through the development of biodegradable polycations (78). We envision that polycations would be particularly useful during initial infection, especially in context of intratumoral injection, in maximizing the number of initially

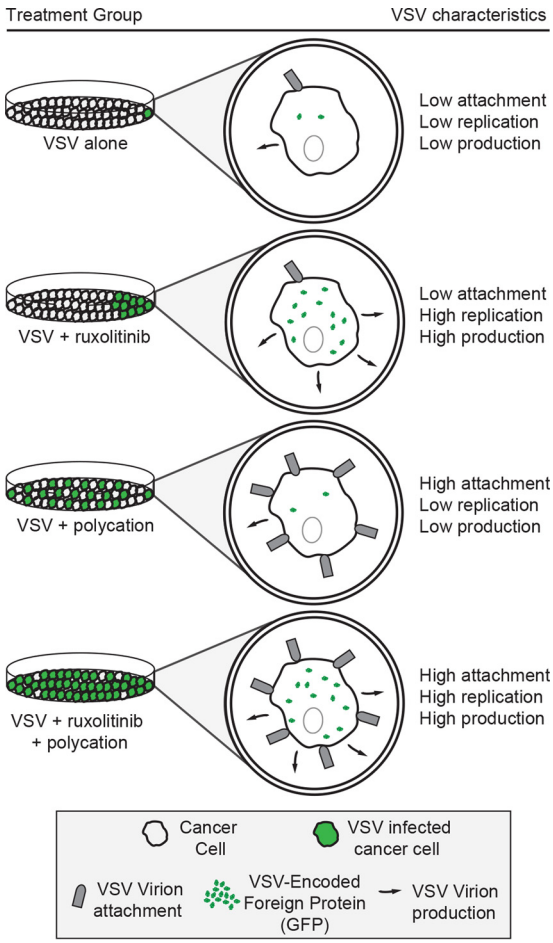

FIG 9 Proposed schematics of breaking resistance of PDAC cells to VSV by treating cells with polycations and ruxolitinib. Treatment conditions are indicated below each well (on the left). Green cells represent infected cancer cells. On the right, the effect of these treatments on VSV characteristics (attachment, replication, and production) is represented.

infected cells, while ruxolitinib would stimulate the replication and spread of the virus within tumors.

With regard to ruxolitinib, this drug was recently approved by the FDA for the treatment of patients with intermediate- or high-risk myelofibrosis (79). It is important to be aware that the inhibition of innate antiviral responses by ruxolitinib or other inhibitors of antiviral responses could potentially result in increased VSV virulence in normal tissues. However, it was recently shown that ruxolitinib enhanced oncolytic VSV treatment *in vivo*, in both subcutaneous as well as orthotopic xenograft mouse models of ovarian cancer, without causing significant additional toxicity (80). Moreover, other combined treatments of VSV and inhibitors of antiviral responses were examined *in vivo* and were also shown to be effective and safe. For example, VSV in combination with rapamycin, the inhibitor of mammalian target of rapamycin (mTOR) (which stimulates type I IFN production via the phosphorylation of its effectors), selectively killed tumor but not normal cells and increased the survival of immunocompetent rats bearing malignant gliomas. In addition, the histone deacetylase (HDAC) inhibitor MS-275 or suberoylanilide hydroxamic acid (SAHA) reversibly compromised host antiviral responses and enhanced the spread of VSV in various cancer types, with no detection of VSV in normal tissues (81–83). Our future *in vivo* experiments will address the efficacy and safety of triple-combination treatment with VSV plus ruxolitinib and a polycation. To fully examine the anticancer abilities and safety of this treatment, it will need to be tested in an immunocompetent *in vivo* system. Unfortunately, our current *in vitro*

system, based on clinically relevant human PDACs, complicates this task, as HPAF-II and other human PDAC cell lines cannot be tested in immunocompetent mice. Also, in our previous study, all tested mouse PDAC cell lines had defective type I IFN signaling and were highly permissive to VSV (84). Currently, we are examining several other mouse PDAC cell lines for their type I IFN status and susceptibility/permissiveness to VSV. Based on this study, we expect to identify VSV-permissive and VSV-resistant mouse PDAC cell lines that could be tested with VSV-ruxolitinib-polycation combinations in an immunocompetent mouse model of PDAC. We envision that this novel triple-combination (VSV-ruxolitinib-polycation) approach could be used in the future to treat PDAC tumors that are highly resistant to OV therapy.

MATERIALS AND METHODS

Viruses and cell lines. Recombinant VSV-ΔM51-eqFP650 (34) and VSV-ΔM51-GFP (31) were described previously. VSV-ΔM51 has a deletion of the methionine at amino acid position 51 of the matrix protein. In addition, VSV-ΔM51-eqFP650 has the near-infrared fluorescent protein ORF (34) and VSV-ΔM51-GFP has the GFP ORF (31) inserted between the VSV G and L genes. For attachment assays, viruses were ultrapurified exactly as previously described (85). The following human PDAC cell lines were used in this study: HPAF-II (ATCC CRL-1997), Hs766T (ATCC HTB-134), MIA PaCa-2 (ATCC CRL-1420), and Suit2 (86). The human origin of all these PDAC cell lines was confirmed by partial sequencing of V-Ki-ras2 Kirsten rat sarcoma viral oncogene homolog (KRAS) and actin. As expected, all PDAC cell lines had a mutation in KRAS, as is typical for PDACs (28, 29). The baby hamster kidney BHK-21 fibroblast cell line (ATCC CCL-10) was used to grow viruses and determine their titers. MIA PaCa-2, Hs766T, and Suit2 cells were maintained in Dulbecco's modified Eagle's medium (DMEM) (catalog number 10-013-CV; Cellgro), while HPAF-II and BHK-21 cells were maintained in modified Eagle's medium (MEM) (catalog number 10-010-CV; Cellgro). All cell growth media were supplemented with 9% FBS (Gibco), 3.4 mM L-glutamine, 900 U/ml penicillin, and 900 μg/ml streptomycin (HyClone). MEM was additionally supplemented with 0.3% (wt/vol) glucose. Cells were kept in a 5% CO_2 atmosphere at 37°C. For all experiments, PDAC cell lines were passaged no more than 15 times.

VSV attachment assay. VSV-ΔM51-eqFP650 was used for all attachment assays. To assay for VSV attachment to cells in suspension, adherent cells were washed one time with PBS and then treated with PBS with 0.2% EDTA or 0.05% trypsin for 30 min to detach them from the surface. DMEM or MEM with 10% FBS was then added for trypsin neutralization, and cells were then washed one time with PBS. Cells were then resuspended in DMEM or MEM (without FBS) and incubated for 1 h at 4°C (the rest of the procedure was done at 4°C) for VSV attachment. After incubation, cells were washed 3 times with PBS to remove any unbound virus. Cells were resuspended in PBS with 2% bovine serum albumin (BSA) and blocked for 10 min, followed by a 1-h incubation with a 1:1,000 dilution of VSV-G antibody (catalog number 8G5F11; Kerafast) and a 30-min incubation with a 1:10 dilution of mouse $F(ab)_2$ IgG(H+L) allophycocyanin (APC)-conjugated antibody (catalog number F0101B; R&D Systems). Cells were analyzed by using the LSR Fortessa cell analyzer (BD Bioscience), and the data were analyzed to determine the percentage of positive cells and the MFI with FlowJo software (TreeStar). The MFI represents the arithmetic mean, so the average fluorescence intensity of cells in the population is displayed on histograms. To assay for VSV attachment to the cell monolayer, cells were seeded into a 6-well or 12-well plate such that confluence was 80% the next day. Medium was then removed, and cells were washed one time with PBS. Virus in DMEM or MEM (without FBS) was then added, and cells were incubated on a rocker for 1 h at 4°C. After incubation, wells were washed 3 times with PBS to remove any unbound virus. Protein isolation buffer was added, and Western blot analysis was performed (as described below).

Protein isolation and Western blot analysis. Cells were seeded into a 6-well or 12-well plate and treated as described above. Medium was removed, and cells were lysed under nonreducing conditions with lysis buffer containing 0.0625 M Tris-HCl (pH 6.8), 10% glycerol, 2% SDS, and 0.02% (wt/vol) bromophenol blue. We used nonreducing conditions, as a reduction of disulfide bridges in the LDLR from the medium was previously reported to prevent the binding of both LDL and the well-characterized LDLR antibodies (87–89). Total protein was separated by electrophoresis on SDS-PAGE gels and electroblotted onto polyvinylidene difluoride membranes. Membranes were blocked by using 5% nonfat powdered milk in TBS-T (0.5 M NaCl, 20 mM Tris [pH 7.5], 0.1% Tween 20). Membranes were incubated with a 1:5,000 dilution of rabbit polyclonal anti-VSV antibodies (raised against VSV virions), a 1:2,000 dilution of anti-LDLR (catalog number AF2148; R&D Systems), or a 1:1,000 dilution of anti-MX1 (catalog number 631-645; Sigma-Aldrich) in TBS-T with 5% BSA or 5% milk with 0.02% sodium azide. Goat anti-mouse, goat anti-rabbit, or chicken anti-goat horseradish peroxidase-conjugated secondary antibodies (Jackson-ImmunoResearch) were used. The Amersham ECL Western blotting detection kit (GE Healthcare) was used for detection. To verify total protein in each loaded sample, membranes were reprobed with a 1:1,000 dilution of rabbit anti-glyceraldehyde-3-phosphate dehydrogenase (GAPDH) antibody (catalog number sc-25778; Santa Cruz) or stained with Coomassie blue R-250.

ELISA. Cells were seeded into a 96-well plate with the appropriate medium (9% FBS) so that they were 80% confluent the next day. The wells were then aspirated, washed one time with PBS, and replaced with the appropriate medium (0% FBS) and treatment. The treatments consisted of dimethyl sulfoxide (DMSO) only, IFN (catalog number 407294-5MU; Calbiochem) (5,000 U/ml), ruxolitinib (INCB018424; Jakafi or Jakavi) (2.5 μM), and an IFN (5,000 U/ml)-ruxolitinib (2.5 μM) mixture in the appropriate medium with 0% FBS. All reaction mixtures contained 0.1% DMSO. Cell culture lysates and

supernatants were isolated 24 h later and analyzed for cellular LDLR and sLDLR, respectively, by an ELISA according to the manufacturer's instructions (Human LDL R Quantikine ELISA kit, catalog number DLDLR0; R&D Systems).

FACS analysis of LDLR cell surface expression. For the LDLR cell surface expression experiment, cells were washed one time with PBS and then incubated with 0.2% EDTA in PBS (to retain LDLR on the cell surface). When the adherent cells detached, cells were counted with a hemocytometer, and 1 million cells were used under each condition. Three conditions were used for each cell line: cells alone, cells with secondary antibody (indicated as "control" in the figures), and cells with primary and secondary antibodies (indicated as "LDLR" in the figures). Cells were not fixed or permeabilized and were incubated at 4°C during the entire procedure. Cells were first blocked in 2% BSA for 10 min and then incubated with a 1:10 dilution of primary antibody against human LDLR (catalog number AF2148; R&D Systems) for 30 min and with a 1:10 dilution of secondary antibody [goat IgG(H+L) APC-conjugated antibody, catalog number F0108; R&D Systems] for 15 min. Cells were washed with PBS one time after incubation with the primary antibody and six times after incubation with the secondary antibody. Cells were analyzed on an LSR Fortessa cell analyzer (BD Bioscience), and the data were analyzed with FlowJo software (TreeStar).

LDL uptake assay. For the LDL uptake assay, cells were seeded into 6-well plates. Medium was then aspirated, wells were washed one time with PBS, and DMEM or MEM with 0% FBS was then added. Fluorescently labeled LDL from human plasma (catalog number L3482; Molecular Probes) was then added to the medium at a concentration of 3 μg/ml for 4 h at 37°C. Medium was then aspirated, and cells were washed 3 times with PBS to remove unbound LDL. Cells were then incubated with 0.05% trypsin in PBS to eliminate LDL that bound but did not enter the cells. Cells were analyzed by using the LSR Fortessa cell analyzer (BD Bioscience), and the data were analyzed with FlowJo software (TreeStar).

Immunofluorescence. For LDLR cell surface expression analysis, cells were seeded into 24-well plates. Cells were not fixed or permeabilized and were incubated at 4°C during the entire procedure. Cells were washed two times with PBS, blocked in 5% BSA for 30 min, and then incubated with a 1:20 dilution of primary antibody against human LDLR (catalog number AF2148; R&D Systems) for 1 h and with a 1:200 dilution of secondary antibody [rabbit anti-goat IgG(H+L) cross-adsorbed secondary antibody, Alexa Fluor 488, catalog number A-11078; Thermo Fisher) for 1 h. Cells were washed with PBS three times after incubation with the primary antibody and after incubation with the secondary antibody. Cell were visualized with an Olympus IX70 instrument, and pictures were taken with an AxioCam HRc camera (Zeiss).

Inhibition of VSV infection by soluble LDLR. To analyze the effect of sLDLR on VSV infectivity, cells were seeded into 12-well plates so that they were 80% confluent the next day. Medium was then aspirated, wells were washed one time with PBS, and DMEM with 0% FBS was then added. sLDLR (catalog number 2148-LD-025; R&D Systems) was first added at a concentration of 1 μg/ml, and VSV-ΔM51-eqFP650 was then added. Cells were incubated with the mixture for 30 min at 37°C. The cells were then washed 3 times with PBS and overlaid with 0.5% agar-containing DMEM (5% FBS). Plaques were counted 16 h later to determine the titer.

Effects of statins on VSV attachment, LDL uptake, and LDLR cell surface expression. Atorvastatin calcium (catalog number S2077), fluvastatin sodium (catalog number S1909), rosuvastatin calcium (catalog number S2169), simvastatin (catalog number S1792), and SBC-115076 (catalog number S7976) (a PCSK9 antagonist) were purchased from Selleck Chemicals. Cells were seeded so that they were 80% confluent (VSV attachment and LDL uptake) or 50% confluent (LDLR cell surface expression) the next day. Medium was then aspirated, the cells were washed one time with PBS, and statins or SBC-115076 was then added at the appropriate concentration in MEM with 5% FBS for 24 h. VSV attachment (monolayer), LDL uptake, or LDLR cell surface expression (FACS and immunofluorescence) assays were performed as described above.

Effects of polycations on VSV infectivity, cell viability, and VSV attachment. HPAF-II cells were seeded into a 96-well plate such that they were approximately 90% confluent at the time of treatment. Cells were washed once with PBS. Under each test condition, various concentrations of DEAE-dextran (catalog number J63781; Alfa Aesar) or Polybrene (catalog number TR-1003-G; Millipore) and protons in MEM without FBS were added to cells. For control wells, MEM without FBS was added. The plate was incubated at 37°C for 30 min, during which it was rocked every 5 min. VSV-ΔM51-GFP in MEM without FBS at an MOI of 0.1, based on the titer determined on HPAF-II cells, was added, and the mixture was incubated for 1 h, with rocking every 10 min. The mixture was aspirated, wells were washed 3 times with PBS, MEM with 5% FBS was added to wells, and cells were incubated at 37°C. GFP fluorescence was measured at regular intervals (CytoFluor series 4000, with an excitation filter of 485 $\pm$ 10 nm, an emission filter of 530 $\pm$ 12.5 nm, and a gain of 63; Applied Biosystems). At 5 days postinfection, cell viability was determined by an MTT cell viability assay (Biotium). For VSV attachment in monolayers, HPAF-II cells were seeded into a 12-well plate such that they were approximately 80% confluent at the time of treatment. Polybrene and DEAE-dextran, both at 10 μg/ml in MEM without FBS, were incubated with cells for 30 min at 4°C. Cells were then incubated with VSV-ΔM51-eqFP650 at an MOI of 250, based on the titer determined on MIA PaCa-2 cells, for 1 h at 4°C. VSV attachment to the monolayer was then monitored as described above. For VSV attachment in suspension, HPAF-II cells were seeded into a T75 flask such that they were approximately 90% confluent at the time of treatment. Cells were washed once with PBS. The flask was incubated for 30 min after the addition of 0.05% trypsin for cell detachment. MEM with 10% FBS was added to neutralize trypsin. Cells were kept at 4°C during cell counting. One million HPAF-II cells were transferred to 1.5-ml tubes for each condition. Polybrene and DEAE-dextran, both at 10 μg/ml in MEM without FBS, were incubated with cells for 30 min, with 5 min between mixes, at 4°C. Cells were then incubated with VSV at an MOI of 125, based on the titer determined on MIA PaCa-2 cells, for 1 h

at 4°C, with 15 min between inversions. VSV attachment to cells in suspension was then monitored as described above. For LDL uptake, HPAF-II cells were seeded into a 6-well plate such that they were approximately 80% confluent at the time of treatment. Polybrene and DEAE-dextran, both at 10 μg/ml in MEM without FBS, were incubated with cells for 30 min at 4°C. Cells were then incubated with fluorescently labeled LDL from human plasma (catalog number L3482; Molecular Probes) at a concentration of 3 μg/ml in medium in the presence of polycations for 4 h at 37°C. The LDL uptake protocol was then performed as described above.

Effects of combinations of polycations and ruxolitinib on VSV infectivity, replication, and cell viability. HPAF-II, Hs766T, MIA PaCa-2, and Suit-2 cells were seeded into a 96-well plate such that they were approximately 80% confluent at the time of treatment. Cells were washed once with PBS. Under each test condition, Polybrene or DEAE-dextran in MEM without FBS was added to cells at a concentration of 10 μg/ml. For control and ruxolitinib wells, MEM without FBS was added. The plate was incubated at 37°C for 30 min, during which it was rocked every 5 min. VSV-ΔM51-GFP in MEM without FBS at a cell line-specific MOI of 0.001 was added, and the plate was incubated for 1 h, with rocking every 10 min. The mixture was aspirated, and wells were washed 3 times with PBS. For ruxolitinib-treated wells, MEM with 5% FBS, 0.1% DMSO, and 2.5 μM ruxolitinib was added. For wells without ruxolitinib treatment, MEM with 5% FBS and 0.1% DMSO was added. The plate was incubated at 37°C. GFP fluorescence was measured at regular intervals (CytoFluor series 4000, with an excitation filter of 485 $\pm$ 10 nm, an emission filter of 530 $\pm$ 12.5 nm, and a gain of 63; Applied Biosystems). A cell viability assay (MTT) was performed at 3 days p.i. To examine the effects of polycations on VSV infectivity by FACS analysis, HPAF-II cells were seeded into a 6-well plate such that they were approximately 80% confluent at the time of treatment. Cells were washed once with PBS. Under each test condition, DEAE-dextran or Polybrene in MEM without FBS at a concentration of 10 μg/ml was dispensed appropriately. For control and ruxolitinib wells, MEM without FBS was added. The plate was incubated at 37°C for 30 min, during which it was rocked every 5 min. VSV-ΔM51-GFP in MEM without FBS at an MOI of 0.001 was added, and the mixture was incubated for 1 h, with rocking every 10 min. The mixture was aspirated, and wells were washed 3 times with PBS. For ruxolitinib-treated wells, MEM with 5% FBS, 0.1% DMSO, and 2.5 μM ruxolitinib was added. For wells without ruxolitinib treatment, MEM with 5% FBS and 0.1% DMSO was added. Wells were incubated at 37°C. At 18 h p.i., cells were washed once with PBS and then trypsinized and resuspended in MEM with 10% FBS. The mixture was transferred to flow cytometry tubes and spun at 2,000 rpm for 2 min. The supernatant was aspirated, and the pellet was washed with PBS and then spun again at 2,000 rpm for 2 min. The pellet was fixed with 500 μl of 4% paraformaldehyde and kept on ice for 15 min. After another round of centrifugation, the pellet was resuspended in PBS and kept on ice. Cells were analyzed on an LSR Fortessa cell analyzer (BD Bioscience), and the data were analyzed with FlowJo software (TreeStar).

Statistical analysis. All statistical analyses were performed by using GraphPad Prism 7.0a software. Tests used are indicated in the legends of the figures.

ACKNOWLEDGMENTS

We are grateful to Eric Hastie and Christian Bressy for critical review of the manuscript. We thank Peter Michaely from UT Southwestern for his help with and expertise on LDLR and Didier Dréau for his help with and expertise on FACS analysis. We are grateful to the following individuals for kindly providing reagents for this project: Jack Rose (Yale University) for VSV-ΔM51-GFP, Pinku Mukherjee (University of North Carolina at Charlotte) for MIA PaCa-2 cells, David McConky (MD Anderson Cancer Center) for Hs766T cells, Andrei Ivanov (University of Rochester Medical School) for HPAF-II cells, and Michael Hollingsworth (University of Nebraska Medical Center) for Suit2 cells.

V.Z.G. is funded by grant 1R15CA195463 from the National Cancer Institute, National Institutes of Health (Bethesda, MD, USA).

REFERENCES

1. Orloff M. 2016. Spotlight on talimogene laherparepvec for the treatment of melanoma lesions in the skin and lymph nodes. Oncolytic Virother 5:91–98. https://doi.org/10.2147/OV.S99532.
2. Rehman H, Silk AW, Kane MP, Kaufman HL. 2016. Into the clinic: talimogene laherparepvec (T-VEC), a first-in-class intratumoral oncolytic viral therapy. J Immunother Cancer 4:53. https://doi.org/10.1186/s40425-016-0158-5.
3. Donina S, Strele I, Proboka G, Auzins J, Alberts P, Jonsson B, Venskus D, Muceniece A. 2015. Adapted ECHO-7 virus Rigvir immunotherapy (oncolytic virotherapy) prolongs survival in melanoma patients after surgical excision of the tumour in a retrospective study. Melanoma Res 25:421–426. https://doi.org/10.1097/CMR.0000000000000180.
4. Garber K. 2006. China approves world's first oncolytic virus therapy for cancer treatment. J Natl Cancer Inst 98:298–300. https://doi.org/10.1093/jnci/djj111.
5. Hastie E, Grdzelishvili VZ. 2012. Vesicular stomatitis virus as a flexible platform for oncolytic virotherapy against cancer. J Gen Virol 93:2529–2545. https://doi.org/10.1099/vir.0.046672-0.
6. Simovic B, Walsh SR, Wan Y. 2015. Mechanistic insights into the oncolytic activity of vesicular stomatitis virus in cancer immunotherapy. Oncolytic Virother 4:157–167. https://doi.org/10.2147/OV.S66079.
7. Hastie E, Cataldi M, Marriott I, Grdzelishvili VZ. 2013. Understanding and altering cell tropism of vesicular stomatitis virus. Virus Res 176:16–32. https://doi.org/10.1016/j.virusres.2013.06.003.
8. Stojdl DF, Lichty BD, Knowles S, Marius R, Atkins H, Sonenberg N, Bell JC. 2000. Exploiting tumor-specific defects in the interferon pathway with a previously unknown oncolytic virus. Nat Med 6:821–825. https://doi.org/10.1038/77558.
9. Stojdl DF, Lichty BD, ten Oever BR, Paterson JM, Power AT, Knowles S, Marius R, Reynard J, Poliquin L, Atkins H, Brown EG, Durbin RK, Durbin JE,

Hiscott J, Bell JC. 2003. VSV strains with defects in their ability to shutdown innate immunity are potent systemic anti-cancer agents. Cancer Cell 4:263–275. https://doi.org/10.1016/S1535-6108(03)00241-1.
10. Lichty BD, Power AT, Stojdl DF, Bell JC. 2004. Vesicular stomatitis virus: re-inventing the bullet. Trends Mol Med 10:210–216. https://doi.org/10.1016/j.molmed.2004.03.003.
11. Barber GN. 2004. Vesicular stomatitis virus as an oncolytic vector. Viral Immunol 17:516–527. https://doi.org/10.1089/vim.2004.17.516.
12. Wang BX, Rahbar R, Fish EN. 2011. Interferon: current status and future prospects in cancer therapy. J Interferon Cytokine Res 31:545–552. https://doi.org/10.1089/jir.2010.0158.
13. Petersen JM, Her LS, Varvel V, Lund E, Dahlberg JE. 2000. The matrix protein of vesicular stomatitis virus inhibits nucleocytoplasmic transport when it is in the nucleus and associated with nuclear pore complexes. Mol Cell Biol 20:8590–8601. https://doi.org/10.1128/MCB.20.22.8590-8601.2000.
14. Clarke DK, Nasar F, Lee M, Johnson JE, Wright K, Calderon P, Guo M, Natuk R, Cooper D, Hendry RM, Udem SA. 2007. Synergistic attenuation of vesicular stomatitis virus by combination of specific G gene truncations and N gene translocations. J Virol 81:2056–2064. https://doi.org/10.1128/JVI.01911-06.
15. Johnson JE, Nasar F, Coleman JW, Price RE, Javadian A, Draper K, Lee M, Reilly PA, Clarke DK, Hendry RM, Udem SA. 2007. Neurovirulence properties of recombinant vesicular stomatitis virus vectors in non-human primates. Virology 360:36–49. https://doi.org/10.1016/j.virol.2006.10.026.
16. Finkelshtein D, Werman A, Novick D, Barak S, Rubinstein M. 2013. LDL receptor and its family members serve as the cellular receptors for vesicular stomatitis virus. Proc Natl Acad Sci U S A 110:7306–7311. https://doi.org/10.1073/pnas.1214441110.
17. Schlegel R, Tralka TS, Willingham MC, Pastan I. 1983. Inhibition of VSV binding and infectivity by phosphatidylserine: is phosphatidylserine a VSV-binding site? Cell 32:639–646. https://doi.org/10.1016/0092-8674(83)90483-X.
18. Coil DA, Miller AD. 2004. Phosphatidylserine is not the cell surface receptor for vesicular stomatitis virus. J Virol 78:10920–10926. https://doi.org/10.1128/JVI.78.20.10920-10926.2004.
19. Carneiro FA, Lapido-Loureiro PA, Cordo SM, Stauffer F, Weissmuller G, Bianconi ML, Juliano MA, Juliano L, Bisch PM, Da Poian AT. 2006. Probing the interaction between vesicular stomatitis virus and phosphatidylserine. Eur Biophys J 35:145–154. https://doi.org/10.1007/s00249-005-0012-z.
20. Schloemer RH, Wagner RR. 1975. Cellular adsorption function of the sialoglycoprotein of vesicular stomatitis virus and its neuraminic acid. J Virol 15:882–893.
21. Guibinga GH, Miyanohara A, Esko JD, Friedmann T. 2002. Cell surface heparan sulfate is a receptor for attachment of envelope protein-free retrovirus-like particles and VSV-G pseudotyped MLV-derived retrovirus vectors to target cells. Mol Ther 5:538–546. https://doi.org/10.1006/mthe.2002.0578.
22. Pearson AS, Koch PE, Atkinson N, Xiong M, Finberg RW, Roth JA, Fang B. 1999. Factors limiting adenovirus-mediated gene transfer into human lung and pancreatic cancer cell lines. Clin Cancer Res 5:4208–4213.
23. Stathis A, Moore MJ. 2010. Advanced pancreatic carcinoma: current treatment and future challenges. Nat Rev Clin Oncol 7:163–172. https://doi.org/10.1038/nrclinonc.2009.236.
24. Rahib L, Smith BD, Aizenberg R, Rosenzweig AB, Fleshman JM, Matrisian LM. 2014. Projecting cancer incidence and deaths to 2030: the unexpected burden of thyroid, liver, and pancreas cancers in the United States. Cancer Res 74:2913–2921. https://doi.org/10.1158/0008-5472.CAN-14-0155.
25. Wennier S, Li S, McFadden G. 2011. Oncolytic virotherapy for pancreatic cancer. Expert Rev Mol Med 13:e18. https://doi.org/10.1017/S1462399411001876.
26. Murphy AM, Besmer DM, Moerdyk-Schauwecker M, Moestl N, Ornelles DA, Mukherjee P, Grdzelishvili VZ. 2012. Vesicular stomatitis virus as an oncolytic agent against pancreatic ductal adenocarcinoma. J Virol 86:3073–3087. https://doi.org/10.1128/JVI.05640-11.
27. Moerdyk-Schauwecker M, Shah NR, Murphy AM, Hastie E, Mukherjee P, Grdzelishvili VZ. 2013. Resistance of pancreatic cancer cells to oncolytic vesicular stomatitis virus: role of type I interferon signaling. Virology 436:221–234. https://doi.org/10.1016/j.virol.2012.11.014.
28. Cataldi M, Shah NR, Felt SA, Grdzelishvili VZ. 2015. Breaking resistance of pancreatic cancer cells to an attenuated vesicular stomatitis virus through a novel activity of IKK inhibitor TPCA-1. Virology 485:340–354. https://doi.org/10.1016/j.virol.2015.08.003.
29. Hastie E, Cataldi M, Moerdyk-Schauwecker MJ, Felt SA, Steuerwald N, Grdzelishvili VZ. 2016. Novel biomarkers of resistance of pancreatic cancer cells to oncolytic vesicular stomatitis virus. Oncotarget 7:61601–61618. https://doi.org/10.18632/oncotarget.11202.
30. Felt SA, Moerdyk-Schauwecker MJ, Grdzelishvili VZ. 2015. Induction of apoptosis in pancreatic cancer cells by vesicular stomatitis virus. Virology 474:163–173. https://doi.org/10.1016/j.virol.2014.10.026.
31. Wollmann G, Rogulin V, Simon I, Rose JK, van den Pol AN. 2010. Some attenuated variants of vesicular stomatitis virus show enhanced oncolytic activity against human glioblastoma cells relative to normal brain cells. J Virol 84:1563–1573. https://doi.org/10.1128/JVI.02040-09.
32. Ahmed M, McKenzie MO, Puckett S, Hojnacki M, Poliquin L, Lyles DS. 2003. Ability of the matrix protein of vesicular stomatitis virus to suppress beta interferon gene expression is genetically correlated with the inhibition of host RNA and protein synthesis. J Virol 77:4646–4657. https://doi.org/10.1128/JVI.77.8.4646-4657.2003.
33. Kopecky SA, Willingham MC, Lyles DS. 2001. Matrix protein and another viral component contribute to induction of apoptosis in cells infected with vesicular stomatitis virus. J Virol 75:12169–12181. https://doi.org/10.1128/JVI.75.24.12169-12181.2001.
34. Hastie E, Cataldi M, Steuerwald N, Grdzelishvili VZ. 2015. An unexpected inhibition of antiviral signaling by virus-encoded tumor suppressor p53 in pancreatic cancer cells. Virology 483:126–140. https://doi.org/10.1016/j.virol.2015.04.017.
35. Ammayappan A, Peng KW, Russell SJ. 2013. Characteristics of oncolytic vesicular stomatitis virus displaying tumor-targeting ligands. J Virol 87:13543–13555. https://doi.org/10.1128/JVI.02240-13.
36. Amirache F, Levy C, Costa C, Mangeot PE, Torbett BE, Wang CX, Negre D, Cosset FL, Verhoeyen E. 2014. Mystery solved: VSV-G-LVs do not allow efficient gene transfer into unstimulated T cells, B cells, and HSCs because they lack the LDL receptor. Blood 123:1422–1424. https://doi.org/10.1182/blood-2013-11-540641.
37. Guillaumond F, Bidaut G, Ouaissi M, Servais S, Gouirand V, Olivares O, Lac S, Borge L, Roques J, Gayet O, Pinault M, Guimaraes C, Nigri J, Loncle C, Lavaut MN, Garcia S, Tailleux A, Staels B, Calvo E, Tomasini R, Iovanna JL, Vasseur S. 2015. Cholesterol uptake disruption, in association with chemotherapy, is a promising combined metabolic therapy for pancreatic adenocarcinoma. Proc Natl Acad Sci U S A 112:2473–2478. https://doi.org/10.1073/pnas.1421601112.
38. Tolleshaug H, Goldstein JL, Schneider WJ, Brown MS. 1982. Posttranslational processing of the LDL receptor and its genetic disruption in familial hypercholesterolemia. Cell 30:715–724. https://doi.org/10.1016/0092-8674(82)90276-8.
39. Tolleshaug H, Hobgood KK, Brown MS, Goldstein JL. 1983. The LDL receptor locus in familial hypercholesterolemia: multiple mutations disrupt transport and processing of a membrane receptor. Cell 32:941–951. https://doi.org/10.1016/0092-8674(83)90079-X.
40. Maxwell KN, Fisher EA, Breslow JL. 2005. Overexpression of PCSK9 accelerates the degradation of the LDLR in a post-endoplasmic reticulum compartment. Proc Natl Acad Sci U S A 102:2069–2074. https://doi.org/10.1073/pnas.0409736102.
41. Marais AD. 2004. Familial hypercholesterolaemia. Clin Biochem Rev 25:49–68.
42. Tveten K, Ranheim T, Berge KE, Leren TP, Kulseth MA. 2006. Analysis of alternatively spliced isoforms of human LDL receptor mRNA. Clin Chim Acta 373:151–157. https://doi.org/10.1016/j.cca.2006.05.031.
43. Pahan K. 2006. Lipid-lowering drugs. Cell Mol Life Sci 63:1165–1178. https://doi.org/10.1007/s00018-005-5406-7.
44. Vaziri ND, Liang K. 2004. Effects of HMG-CoA reductase inhibition on hepatic expression of key cholesterol-regulatory enzymes and receptors in nephrotic syndrome. Am J Nephrol 24:606–613. https://doi.org/10.1159/000082510.
45. Santos RD, Watts GF. 2015. Familial hypercholesterolaemia: PCSK9 inhibitors are coming. Lancet 385:307–310. https://doi.org/10.1016/S0140-6736(14)61702-5.
46. McNutt MC, Kwon HJ, Chen C, Chen JR, Horton JD, Lagace TA. 2009. Antagonism of secreted PCSK9 increases low density lipoprotein receptor expression in HepG2 cells. J Biol Chem 284:10561–10570. https://doi.org/10.1074/jbc.M808802200.
47. Wu M, Dong B, Cao A, Li H, Liu J. 2012. Delineation of molecular pathways that regulate hepatic PCSK9 and LDL receptor expression

during fasting in normolipidemic hamsters. Atherosclerosis 224: 401–410. https://doi.org/10.1016/j.atherosclerosis.2012.08.012.
48. Chen Y, Ruan XZ, Li Q, Huang A, Moorhead JF, Powis SH, Varghese Z. 2007. Inflammatory cytokines disrupt LDL-receptor feedback regulation and cause statin resistance: a comparative study in human hepatic cells and mesangial cells. Am J Physiol Renal Physiol 293:F680–F687. https://doi.org/10.1152/ajprenal.00209.2007.
49. Ye Q, Lei H, Fan Z, Zheng W, Zheng S. 2014. Difference in LDL receptor feedback regulation in macrophages and vascular smooth muscle cells: foam cell transformation under inflammatory stress. Inflammation 37: 555–565. https://doi.org/10.1007/s10753-013-9769-x.
50. Russell DW, Yamamoto T, Schneider WJ, Slaughter CJ, Brown MS, Goldstein JL. 1983. cDNA cloning of the bovine low density lipoprotein receptor: feedback regulation of a receptor mRNA. Proc Natl Acad Sci U S A 80:7501–7505. https://doi.org/10.1073/pnas.80.24.7501.
51. Fischer DG, Novick D, Cohen B, Rubinstein M. 1994. Isolation and characterization of a soluble form of the LDL receptor, an interferon-induced antiviral protein. Proc Soc Exp Biol Med 206:228–232. https://doi.org/10.3181/00379727-206-43749.
52. Fischer DG, Tal N, Novick D, Barak S, Rubinstein M. 1993. An antiviral soluble form of the LDL receptor induced by interferon. Science 262: 250–253. https://doi.org/10.1126/science.8211145.
53. Kniss DA, Summerfield TL. 2014. Discovery of HeLa cell contamination in HES cells: call for cell line authentication in reproductive biology. Res Reprod Sci 21:1015–1019. https://doi.org/10.1177/1933719114522518.
54. Kingsley DM, Kozarsky KF, Hobbie L, Krieger M. 1986. Reversible defects in O-linked glycosylation and LDL receptor expression in a UDP-Gal/UDP-GalNAc 4-epimerase deficient mutant. Cell 44:749–759. https://doi.org/10.1016/0092-8674(86)90841-X.
55. Kozarsky K, Kingsley D, Krieger M. 1988. Use of a mutant cell line to study the kinetics and function of O-linked glycosylation of low density lipoprotein receptors. Proc Natl Acad Sci U S A 85:4335–4339. https://doi.org/10.1073/pnas.85.12.4335.
56. Conti C, Mastromarino P, Riccioli A, Orsi N. 1991. Electrostatic interactions in the early events of VSV infection. Res Virol 142:17–24. https://doi.org/10.1016/0923-2516(91)90023-V.
57. Bailey CA, Miller DK, Lenard J. 1984. Effects of DEAE-dextran on infection and hemolysis by VSV. Evidence that nonspecific electrostatic interactions mediate effective binding of VSV to cells. Virology 133:111–118. https://doi.org/10.1016/0042-6822(84)90429-X.
58. Matlin KS, Reggio H, Helenius A, Simons K. 1982. Pathway of vesicular stomatitis virus entry leading to infection. J Mol Biol 156:609–631. https://doi.org/10.1016/0022-2836(82)90269-8.
59. Reiser J, Harmison G, Kluepfel-Stahl S, Brady RO, Karlsson S, Schubert M. 1996. Transduction of nondividing cells using pseudotyped defective high-titer HIV type 1 particles. Proc Natl Acad Sci U S A 93:15266–15271. https://doi.org/10.1073/pnas.93.26.15266.
60. Yee JK, Friedmann T, Burns JC. 1994. Generation of high-titer pseudotyped retroviral vectors with very broad host range. Methods Cell Biol 43(Part A):99–112. https://doi.org/10.1016/S0091-679X(08)60600-7.
61. Denning W, Das S, Guo S, Xu J, Kappes JC, Hel Z. 2013. Optimization of the transductional efficiency of lentiviral vectors: effect of sera and polycations. Mol Biotechnol 53:308–314. https://doi.org/10.1007/s12033-012-9528-5.
62. Davis CG, Elhammer A, Russell DW, Schneider WJ, Kornfeld S, Brown MS, Goldstein JL. 1986. Deletion of clustered O-linked carbohydrates does not impair function of low density lipoprotein receptor in transfected fibroblasts. J Biol Chem 261:2828–2838.
63. Yoshimura A, Yoshida T, Seguchi T, Waki M, Ono M, Kuwano M. 1987. Low binding capacity and altered O-linked glycosylation of low density lipoprotein receptor in a monensin-resistant mutant of Chinese hamster ovary cells. J Biol Chem 262:13299–13308.
64. Kalra AV, Campbell RB. 2009. Mucin overexpression limits the effectiveness of 5-FU by reducing intracellular drug uptake and antineoplastic drug effects in pancreatic tumours. Eur J Cancer 45:164–173. https://doi.org/10.1016/j.ejca.2008.10.008.
65. Kalra AV, Campbell RB. 2007. Mucin impedes cytotoxic effect of 5-FU against growth of human pancreatic cancer cells: overcoming cellular barriers for therapeutic gain. Br J Cancer 97:910–918. https://doi.org/10.1038/sj.bjc.6603972.
66. Davis HE, Morgan JR, Yarmush ML. 2002. Polybrene increases retrovirus gene transfer efficiency by enhancing receptor-independent virus adsorption on target cell membranes. Biophys Chem 97:159–172. https://doi.org/10.1016/S0301-4622(02)00057-1.
67. Tiera MJ, Shi Q, Winnik FM, Fernandes JC. 2011. Polycation-based gene therapy: current knowledge and new perspectives. Curr Gene Ther 11:288–306. https://doi.org/10.2174/156652311796150408.
68. Aied A, Greiser U, Pandit A, Wang W. 2013. Polymer gene delivery: overcoming the obstacles. Drug Discov Today 18:1090–1098. https://doi.org/10.1016/j.drudis.2013.06.014.
69. Kaplan JM, Pennington SE, St George JA, Woodworth LA, Fasbender A, Marshall J, Cheng SH, Wadsworth SC, Gregory RJ, Smith AE. 1998. Potentiation of gene transfer to the mouse lung by complexes of adenovirus vector and polycations improves therapeutic potential. Hum Gene Ther 9:1469–1479. https://doi.org/10.1089/hum.1998.9.10-1469.
70. McKay TR, MacVinish LJ, Carpenter B, Themis M, Jezzard S, Goldin R, Pavirani A, Hickman ME, Cuthbert AW, Coutelle C. 2000. Selective in vivo transfection of murine biliary epithelia using polycation-enhanced adenovirus. Gene Ther 7:644–652. https://doi.org/10.1038/sj.gt.3301144.
71. Gregory LG, Harbottle RP, Lawrence L, Knapton HJ, Themis M, Coutelle C. 2003. Enhancement of adenovirus-mediated gene transfer to the airways by DEAE dextran and sodium caprate in vivo. Mol Ther 7:19–26. https://doi.org/10.1016/S1525-0016(02)00021-7.
72. Kushwah R, Oliver JR, Cao H, Hu J. 2007. Nacystelyn enhances adenoviral vector-mediated gene delivery to mouse airways. Gene Ther 14: 1243–1248. https://doi.org/10.1038/sj.gt.3302968.
73. Monnery BD, Wright M, Cavill R, Hoogenboom R, Shaunak S, Steinke JH, Thanou M. 2017. Cytotoxicity of polycations: relationship of molecular weight and the hydrolytic theory of the mechanism of toxicity. Int J Pharm 521:249–258. https://doi.org/10.1016/j.ijpharm.2017.02.048.
74. Zarogoulidis P, Hohenforst-Schmidt W, Darwiche K, Krauss L, Sparopoulou D, Sakkas L, Gschwendtner A, Huang H, Turner FJ, Freitag L, Zarogoulidis K. 2013. 2-Diethylaminoethyl-dextran methyl methacrylate copolymer nonviral vector: still a long way toward the safety of aerosol gene therapy. Gene Ther 20:1022–1028. https://doi.org/10.1038/gt.2013.27.
75. Simmons CF, Jr, Rennke HG, Humes HD. 1981. Acute renal failure induced by diethylaminoethyl dextran: importance of cationic charge. Kidney Int 19:424–430. https://doi.org/10.1038/ki.1981.35.
76. Seitz B, Baktanian E, Gordon EM, Anderson WF, LaBree L, McDonnell PJ. 1998. Retroviral vector-mediated gene transfer into keratocytes: in vitro effects of Polybrene and protamine sulfate. Graefes Arch Clin Exp Ophthalmol 236:602–612. https://doi.org/10.1007/s004170050129.
77. Lin P, Correa D, Lin Y, Caplan AI. 2011. Polybrene inhibits human mesenchymal stem cell proliferation during lentiviral transduction. PLoS One 6:e23891. https://doi.org/10.1371/journal.pone.0023891.
78. Park TG, Jeong JH, Kim SW. 2006. Current status of polymeric gene delivery systems. Adv Drug Deliv Rev 58:467–486. https://doi.org/10.1016/j.addr.2006.03.007.
79. Vaddi K, Sarlis NJ, Gupta V. 2012. Ruxolitinib, an oral JAK1 and JAK2 inhibitor, in myelofibrosis. Expert Opin Pharmacother 13:2397–2407. https://doi.org/10.1517/14656566.2012.732998.
80. Dold C, Rodriguez Urbiola C, Wollmann G, Egerer L, Muik A, Bellmann L, Fiegl H, Marth C, Kimpel J, von Laer D. 2016. Application of interferon modulators to overcome partial resistance of human ovarian cancers to VSV-GP oncolytic viral therapy. Mol Ther Oncolytics 3:16021. https://doi.org/10.1038/mto.2016.21.
81. Nguyên TL, Abdelbary H, Arguello M, Breitbach C, Leveille S, Diallo JS, Yasmeen A, Bismar TA, Kirn D, Falls T, Snoulten VE, Vanderhyden BC, Werier J, Atkins H, Vähä-Koskela MJ, Stojdl DF, Bell JC, Hiscott J. 2008. Chemical targeting of the innate antiviral response by histone deacetylase inhibitors renders refractory cancers sensitive to viral oncolysis. Proc Natl Acad Sci U S A 105:14981–14986. https://doi.org/10.1073/pnas.0803988105.
82. Shulak L, Beljanski V, Chiang C, Dutta SM, Van Grevenynghe J, Belgnaoui SM, Nguyen TL, Di Lenardo T, Semmes OJ, Lin R, Hiscott J. 2014. Histone deacetylase inhibitors potentiate vesicular stomatitis virus oncolysis in prostate cancer cells by modulating NF-kappaB-dependent autophagy. J Virol 88:2927–2940. https://doi.org/10.1128/JVI.03406-13.
83. Shestakova E, Bandu MT, Doly J, Bonnefoy E. 2001. Inhibition of histone deacetylation induces constitutive derepression of the beta interferon promoter and confers antiviral activity. J Virol 75:3444–3452. https://doi.org/10.1128/JVI.75.7.3444-3452.2001.
84. Hastie E, Besmer DM, Shah NR, Murphy AM, Moerdyk-Schauwecker M, Molestina C, Roy LD, Curry JM, Mukherjee P, Grdzelishvili VZ. 2013. Oncolytic vesicular stomatitis virus in an immunocompetent model of MUC1-positive or MUC1-null pancreatic ductal adenocarcinoma. J Virol 87:10283–10294. https://doi.org/10.1128/JVI.01412-13.
85. Moerdyk-Schauwecker M, Hwang SI, Grdzelishvili VZ. 2014. Cellular pro-

teins associated with the interior and exterior of vesicular stomatitis virus virions. PLoS One 9:e104688. https://doi.org/10.1371/journal.pone.0104688.
86. Iwamura T, Katsuki T, Ide K. 1987. Establishment and characterization of a human pancreatic cancer cell line (SUIT-2) producing carcinoembryonic antigen and carbohydrate antigen 19-9. Jpn J Cancer Res 78:54–62.
87. Nguyen AT, Hirama T, Chauhan V, Mackenzie R, Milne R. 2006. Binding characteristics of a panel of monoclonal antibodies against the ligand binding domain of the human LDLr. J Lipid Res 47:1399–1405. https://doi.org/10.1194/jlr.M600130-JLR200.
88. Beisiegel U, Schneider WJ, Brown MS, Goldstein JL. 1982. Immunoblot analysis of low density lipoprotein receptors in fibroblasts from subjects with familial hypercholesterolemia. J Biol Chem 257:13150–13156.
89. van Driel IR, Goldstein JL, Sudhof TC, Brown MS. 1987. First cysteine-rich repeat in ligand-binding domain of low density lipoprotein receptor binds Ca2+ and monoclonal antibodies, but not lipoproteins. J Biol Chem 262:17443–17449.